IEEE Access
Multidisciplinary ⋮ Rapid Review ⋮ Open Access Journal

Received 14 June 2024, accepted 5 July 2024, date of publication 11 July 2024, date of current version 19 July 2024.

Digital Object Identifier 10.1109/ACCESS.2024.3426556

RESEARCH ARTICLE

Relay Selection for Full-Duplex Buffer-Aided Relaying

CHADI ABOU-RJEILY, (Senior Member, IEEE)
Department of Electrical and Computer Engineering, Lebanese American University (LAU), Byblos 1102-2801, Lebanon
e-mail: chadi.abourjeily@lau.edu.lb

ABSTRACT In this paper, we consider buffer-aided (BA) relaying with full-duplex (FD) relays. The ability of the FD relays to simultaneously transmit and receive offers new degrees of freedom in the design of BA relay selection strategies. We take this feature into consideration to propose two novel FD BA relay selection schemes. A Markov chain analysis is presented to evaluate the outage probabilities (OP) and average packet delays (APD) of the proposed schemes over generalized $\kappa - \mu$ fading channels. Through an asymptotic analysis, we derive closed-form expressions of the asymptotic OP and APD. This analysis highlights on the impact of the buffer size, number of relays and network architecture on the system performance and allows to draw conclusions on the most suitable scheme to apply in each network setup. Results demonstrate significant performance gains compared to the state-of-the-art half-duplex (HD) BA relaying schemes. In particular, the first proposed scheme is appealing since it minimizes the OP when the relays are closer to the destination while the second scheme achieves an asymptotic APD value of one in this scenario. This highlights on the advantages of FD BA relaying since none of the existing HD BA relaying strategies can achieve an APD below two.

INDEX TERMS Asymptotic analysis, buffer, cooperative networks, data queue, Markov chain, outage probability, performance analysis, queuing delay, relaying.

I. INTRODUCTION

Relaying technologies are pivotal for leveraging the throughput, reliability and coverage of the fifth-generation (5G) wireless networks. These technologies are constantly maturing to meet the Quality-of-Service (QoS) demands of the emerging 5G applications including the Internet-of-Things (IoT), Machine-to-Machine (M2M) communications and vehicular communications [1]. The relaying strategies have evolved from being buffer-free (BF) to become buffer-aided (BA) with storage capabilities enabled at the relays which allow for a more flexible activation of the source-to-relay (S-R) and relay-to-destination (R-D) links in each transmission interval. This flexibility circumvents the transmission along weak hops resulting in an improved outage performance at the expense of incurring queuing delays [2].

BA relay selection was studied with half-duplex (HD) relays that can only transmit and receive in different time slots or orthogonal frequency bands [3], [4], [5]. Also, the problem of BA relaying was tackled with full-duplex (FD) relays that can simultaneously transmit and receive in the same frequency band [6], [7], [8], [9], [10], [11], [12], [13]. While FD communications enhance the multiplexing gain, they suffer from self-interference (SI) due to the energy leaking from the transmitting-end to the receiving-end. However, several SI mitigation techniques have been recently developed and proven to be effective in reducing the SI by around 120 dB [14]. As such, SI is not really problematic to FD relaying and this kind of interference is usually neglected.

K-relay HD BA relay selection was studied in [3], [4], and [5]. The *max-link* scheme in [3] activates the strongest link among all available S-R and R-D links allowing to achieve a diversity order (DO) of $2K$ over Rayleigh fading channels with infinite-size buffers. This maximum DO was achieved with finite-size buffers in [4] by including the actual numbers of packets stored in the relays' buffers in the relay selection procedure. Recently, threshold-based relaying was

The associate editor coordinating the review of this manuscript and approving it for publication was Jiayi Zhang.

advised in [5] where adjustable threshold levels are selected at the relays allowing to achieve different levels of tradeoff between outage probability (OP) and average packet delay (APD). In particular, over Rayleigh fading channels, the thresholds can be tuned to achieve the maximum DO of $2K$ at the expense of an increased asymptotic APD value of $2K + 2$ and to achieve the smallest APD value of 2 with a reduced DO of K [5]. In this context, the asymptotic APD value of 2 is the smallest queuing delay reported in the literature on HD BA relaying and HD relays cannot deliver the packets to D with an average delay below two time slots. As such, the first question that arises is *"can FD BA relaying further reduce the asymptotic APD below 2 owing to the capability of the relays to concurrently transmit and receive?"*

The problem of FD BA relaying was studied in [6] with a single relay equipped with an infinite-size buffer. The optimization problem revolved around maximizing the rate for a communication session that extends over an infinite number of symbol durations where various power and rate allocation schemes were considered. The FD BA relay can switch between the transmission, reception and simultaneous transmission-reception modes. This flexibility resulted in significant performance gains compared to FD BF systems where the relay always transmits and receives and compared to HD BA systems where the relay cannot simultaneously transmit and receive. An analogous approach of maximizing the average end-to-end data rate over a sufficiently large number of time slots was adopted in [7] and [8]. While conventional FD relaying was considered in [6], this type of relaying was mimicked in [7] using HD relays where the source and a relay are allowed to concurrently transmit in order to compensate for the multiplexing-gain losses incurred by the HD constraint. The inter-relay interference surfacing from the virtual FD BA relaying approach was reduced by deploying multiple antennas at the relays and implementing beamforming techniques. Substantial performance gains were reported with infinite-size buffers while these gains are less pronounced with buffers of finite size less than fifty. While the S-D link was assumed to be unavailable in [6] and [7], the authors of [8] considered additional operation modes in their relaying protocol including direct S-D transmissions, cooperative transmission from the source and a relay and competitive transmission from two relays. In order to simplify the analysis, infinite-size buffers were considered in [8] as well. The works in [9] and [10] included a statistical delay constraint in characterizing the maximum effective capacity (i.e. the maximum supportable source arrival rate) of a three-node cooperative network. Both [9] and [10] considered a FD relay equipped with an infinite-size buffer. While the system model in [9] assumed fixed transmit powers and negligible SI in the presence of a direct link, adaptive power allocation was studied in [10] with non-zero ISI and no direct link. [11] tackled rate adaptation and antenna selection in the case of a single FD relay equipped with multiple antennas and an infinite-size buffer in the absence of a direct link. The antennas at the relay were partitioned into two groups dedicated for reception and transmission where the advised rate adaptation and antenna selection algorithms depend on four states of the buffer; namely, critically empty, critically full, less than half-full and more than half-full. While [6], [7], [8], [9], [10], and [11] considered systems with one source and one destination, FD BA relaying techniques were extended to more general network setups in [12] and [13]. The authors of [12] considered the case of one source node and two destination nodes served by FD relays that implement non-orthogonal multiple access (NOMA). Multi-user scheduling was studied in [13] where the communications between N source-destination pairs take place through a FD relay equipped with N buffers.

The existing FD BA systems considered mainly infinite-size buffers or very large buffers [6], [7], [8], [9], [10], [11]. Not only this assumption is unrealistic in practice, but also the excessive queuing of the packets in the relays' buffers incurs unbounded delays. As such, a second important question to ask is *"how can FD BA relaying be envisaged with finite-size buffers and how can this size be optimized to reduce the delays without compromising the reliability of the network?"* The open literature includes numerous slot-by-slot HD BA relaying schemes where the decision on the link to be activated is made in each time slot [3], [4], [5]. However, to the author's best knowledge, such slot-by-slot strategies are still missing in the context of FD BA relaying and the existing strategies often target maximizing the average throughput for infinitely-long communication sessions [6], [7], [8]. Slot-by-slot relaying strategies are more practical since they are simpler to implement and require less signaling overhead, hence, the third question that arises is *"how can we design a slot-by-slot FD BA relaying scheme that improves on the existing HD BA protocols?"*

This paper aims to answer the above raised questions and makes the following contributions to the existing literature. (i): We propose two novel FD BA relay selection schemes denoted by scheme 1 and scheme 2. As [3], [4], and [5], these schemes can be implemented in a slot-by-slot basis and, unlike [6], [7], [8], [9], [10], and [11], these schemes are adapted to finite-size buffers. (ii): Through a Markov chain analysis, we derive closed-form expressions that relate the achievable asymptotic OP and APD values to the number of relays, buffer size and outage probabilities of the links. (iii): Owing to the tractability of the derived asymptotic performance metrics, we draw conclusions on how to select the buffer size and on which relaying scheme to implement for different network setups. In particular, we prove that a buffer size of two is sufficient for reaping the full potential of the network. When the relays are closer to D, scheme 1 and scheme 2 should be applied if the OP and APD are prioritized, respectively. When the relays are closer to S, scheme 2 achieves a smaller OP compared to scheme 1 with the same APD value rendering scheme 2 the adequate choice for this setup. (iv): We demonstrate the theoretical analysis via Monte Carlo simulations over the generalized $\kappa - \mu$ fading channels. We prove that FD BA relaying can concurrently improve the

outage and delay performances compared to HD BA relaying and we prove that asymptotic APDs below the reference value of 2 can be achieved. In particular, scheme 2 achieves an advantageously small asymptotic APD of 1 regardless of the number of relays when these relays are closer to D.

II. SYSTEM MODEL AND RELAYING STRATEGIES

A. SYSTEM MODEL

Consider a decode-and-forward (DF) cooperative network comprising a source node (S), a destination node (D) and K relays denoted by $\mathrm{R}_1, \ldots, \mathrm{R}_K$. We assume that no direct link is available between S and D and, hence, S communicates with D through the cluster of relays. The signals received at D and the relays are corrupted by an additive white Gaussian noise (AWGN) with zero mean and unit variance. We denote by h_{SR_k} and $h_{\mathrm{R}_k\mathrm{D}}$ the channel coefficients of the S-R_k and R_k-D links, respectively, for $k = 1, \ldots, K$.

A communication link is in outage if the corresponding channel capacity falls below a fixed target rate r_0 (in bits per channel use (BPCU)). As such, the outage probability along the R_k-D link can be determined from $\mathfrak{q}_k = \Pr\left\{\frac{1}{2}\log_2(1+\bar{\gamma}|h_{R_kD}|^2) \leq r_0\right\}$ where $\bar{\gamma}$ stands for the average transmit signal-to-noise ratio (SNR). With the recent advancements in SI cancellation techniques, the residual SI at the FD relays is usually limited. The residual SI is assumed to be zero-mean, additive and Gaussian with a variance that is proportional to the relay transmit power [10]. Assuming the same transmit power at the source and relays and normalizing this power to unity implies that the outage probability along the S-R_k link can be determined from $\mathfrak{p}_k = \Pr\left\{\frac{1}{2}\log_2(1+\frac{\bar{\gamma}}{\beta+1}|h_{SR_k}|^2) \leq r_0\right\}$. In this expression, the parameter $\beta \geq 0$ captures the quality of SI cancellation where a better SI cancellation performance reflects into smaller values of β. Note that, in the expressions of $\mathfrak{q}_k$ and $\mathfrak{p}_k$, the factor $1/2$ is introduced since the communication between S and D is carried out in two time slots. In this work, we adopt the generalized $\kappa-\mu$ fading model due to its wide applicability and generality [15]. The $\kappa-\mu$ distribution encompasses many well known fading models as special cases including the Rice, Nakagami-m, Rayleigh and one-sided Gaussian distributions. Solving for the outage probabilities results in [15]:

$$\mathfrak{p}_k = 1 - Q_{\mu_{SR_k}}\left(\sqrt{2\kappa_{SR_k}\mu_{SR_k}}, \sqrt{2\mathfrak{r}\mu_{SR_k}(1+\kappa_{SR_k})(\Omega_{SR_k}\frac{\bar{\gamma}}{\beta+1})^{-1}}\right) \quad (1)$$

$$\mathfrak{q}_k = 1 - Q_{\mu_{R_kD}}\left(\sqrt{2\kappa_{R_kD}\mu_{R_kD}}, \sqrt{2\mathfrak{r}\mu_{R_kD}(1+\kappa_{R_kD})(\Omega_{R_kD}\bar{\gamma})^{-1}}\right), \quad (2)$$

where $Q_m(\cdot,\cdot)$ stands for the generalized Marcum Q-function while $\mathfrak{r} \triangleq 2^{2r_0}-1$. In (1)-(2), $(\kappa_{SR_k}, \mu_{SR_k})$ and $(\kappa_{R_kD}, \mu_{R_kD})$ stand for the parameters of the $\kappa-\mu$ distributions associated with the S-R_k and R_k-D links, respectively. The parameter κ describes the ratio between the powers of the dominant and scattered waves while μ denotes the number of multi-path clusters. Finally, $\Omega_{SR_k} = \mathrm{E}[|h_{\mathrm{SR}_k}|^2]$ and $\Omega_{R_kD} = \mathrm{E}[|h_{\mathrm{R}_k\mathrm{D}}|^2]$. Note that the eventual presence of residual SI ($\beta \neq 0$) only incurs an increase in the values of the outage probabilities $\{\mathfrak{p}_k\}_{k=1}^K$ without impacting the design of the relaying strategy and the associated performance analysis. In this context, the SI cancellation techniques usually adopted in buffer-free systems can be readily applied in buffer-aided systems.

We assume that the relays are equipped with buffers (data queues) of finite-size L and we denote by $l_k \in \{0, \ldots, L\}$ the number of packets stored in the buffer of R_k for $k = 1, \ldots, K$. A S-R_k link is unavailable if either it is in outage or the buffer at R_k is full so that the incoming packet cannot be stored. Similarly, a R_k-D link is unavailable if either this link is in outage or the buffer at R_k is empty so that no packet can be extracted for transmission. As such, the unavailability probabilities of the S-R_k and R_k-D links can be determined from:

$$p_k = \mathfrak{p}_k + \delta_{l_k=L} - \mathfrak{p}_k\delta_{l_k=L} \quad (3)$$

$$q_k = \mathfrak{q}_k + \delta_{l_k=0} - \mathfrak{q}_k\delta_{l_k=0}, \quad (4)$$

where $\delta_{\mathcal{S}} = 1$ if the statement S is true and $\delta_{\mathcal{S}} = 0$ otherwise.

Note that when the buffer at R_k is not empty, $\delta_{l_k=0} = 0$ implying that $q_k = \mathfrak{q}_k$ from (4). In this case, an outage event along the link R_k-D will render this link unavailable. In other words, despite the fact that R_k has packets to transmit, yet the link R_k-D might be in outage implying that this link will not be selected for activation. Similarly, when the buffer at R_k is not full, $\delta_{l_k=L} = 0$ and $p_k = \mathfrak{p}_k$ from (3) implying that link S-R_k will be available for selection only if it is not in outage.

B. RELAYING STRATEGIES

This work proposes two relaying strategies for FD BA cooperative networks. Both schemes give the highest priority to the activation of an available end-to-end S-R-D link. In other words, if both S-R_k and R_k-D links are available for any $k \in \{1, \ldots, K\}$, then these two links are concurrently activated where the FD relay R_k receives a packet from S while simultaneously transmitting a packet to D. This concurrent activation of two links that pass through the same relay is expected to expedite the flow of packets from S to D, thus, enhancing the network throughput. In fact, selecting the same relay to concurrently transmit and receive will ensure the delivery of a packet to D while keeping the numbers of packets stored in the relays' buffers the same which positively contributes to reducing the queuing delays. With the highest priority granted by the two proposed schemes to the available end-to-end link, these schemes differ by the way they handle the relay selection in the absence of the aforementioned availability. When an end-to-end link is not available, the first scheme randomly activates any one of the available S-R or R-D links while the second scheme prioritizes R-D links over S-R links.

Denote by $\mathcal{C}_t \triangleq \{i \mid \text{R}_i\text{-D not in outage } \& \ l_i \neq 0\}$ and $\mathcal{C}_r \triangleq \{i \mid \text{S-R}_i \text{ not in outage } \& \ l_i \neq L\}$ the sets of relays that are available for transmission and reception, respectively. Denote by $\mathcal{C}_{t,r} = \mathcal{C}_t \cap \mathcal{C}_r$ the set of relays that can simultaneously transmit and receive. The priority orders for scheme 1 are as follows:

1) If $\mathcal{C}_{t,r}$ is not empty, select any relay in this set to simultaneously transmit a packet to D and receive a packet from S.
2) If $\mathcal{C}_{t,r}$ is empty, randomly select a relay either from $\mathcal{C}_t$ to transmit or from $\mathcal{C}_r$ to receive.

The priority orders for scheme 2 are as follows:

1) If $\mathcal{C}_{t,r}$ is not empty, select any relay in this set to simultaneously transmit and receive.
2) If $\mathcal{C}_{t,r}$ is empty and $\mathcal{C}_t$ is not empty, randomly select a relay from $\mathcal{C}_t$ to transmit.
3) If $\mathcal{C}_{t,r}$ and $\mathcal{C}_t$ are empty while $\mathcal{C}_r$ is not empty, randomly select a relay from $\mathcal{C}_r$ to receive.

Scheme 1 and scheme 2 are better represented in Algorithm 1 and Algorithm 2, respectively, where the notation $x \in_R \mathcal{S}$ means that the element x is randomly selected from the set $\mathcal{S}$.

Algorithm 1 Scheme 1

```
Data: C_t and C_r;
Result: Link(s) to be activated;
initialization: No link is activated;
C_{t,r} = C_t ∩ C_r;
  if C_t ∪ C_r ≠ φ then
    if C_{t,r} ≠ φ then
      k ∈_R C_{t,r};
      Activate links S-R_k and R_k-D
    else
      k ∈_R C_t ∪ C_r;
      if k ∈ C_t then
        Activate link R_k-D
      else
        Activate link S-R_k
      end if
    end if
  end if
```

Algorithm 2 Scheme 2

```
Data: C_t and C_r;
Result: Link(s) to be activated;
initialization: No link is activated;
C_{t,r} = C_t ∩ C_r;
  if C_t ∪ C_r ≠ φ then
    if C_{t,r} ≠ φ then
      k ∈_R C_{t,r};
      Activate links S-R_k and R_k-D
    else
      if C_t ≠ φ then
        k ∈_R C_t;
        Activate link R_k-D
      else
        k ∈_R C_r;
        Activate link S-R_k
      end if
    end if
  end if
```

It is worth noting the following. (i): When the two (resp. three) selection steps of scheme 1 (resp. scheme 2) do not yield to the selection of a relay, then no packets are communicated along any of the links of the network that will subsequently be in outage. (ii): When $\mathcal{C}_{t,r} \neq \phi$, the selection of any relay in this set to concurrently transmit and receive is as good as any other selection and, as such, for both schemes the first step randomly selects a relay from this set. In fact, the activations of any one of the links S-R$_k$-D or S-R$_{k'}$-D for $k, k' \in \mathcal{C}_{t,r}$ are equivalent since in both cases a packet is delivered to D while the numbers of packets stored in the relays' buffers remain unchanged. (iii): When all end-to-end links are unavailable, scheme 2 prioritizes transmission over reception while scheme 1 does not favor any of these two operating modes. Prioritizing the transmission contributes to emptying the buffers at a faster pace which advantageously reduces the queuing delays while negatively impacting the availability of the R-D links since a relay with an empty buffer cannot transmit. The pros and cons of prioritizing transmission over reception will be discussed in more details in the subsequent sections.

The implementation of the proposed FD BA relaying schemes does not require the acquisition of the values of the path gains $\{h_{SR_k}, h_{R_kD}\}_{k=1}^{K}$ (as in [3]) or the buffer lengths $\{l_k\}_{k=1}^{K}$ (as in [4], [5]). In this context, only the availabilities of the $2K$ S-R and R-D links need to be acquired. This constitutes a major advantage of the proposed relaying schemes for the following reasons. (i): Limiting the signaling overhead: the channel coefficients $\{h_{SR_k}, h_{R_kD}\}_{k=1}^{K}$ are real-valued. As such, these values need to be quantized and converted into bits for inclusion in the signaling packets. Assuming that each path gain is quantized over $n_q = 2^{n_b}$ levels, then a relaying protocol that includes the path gains in its decision-making process will involve exchanging signaling packets of length $2Kn_b$ where n_b is the number of bits for representing each one of the n_q quantization levels. In general, n_q (and, consequently, n_b) should be large enough for the sake of accurate representation of the path gains implying long signaling packets and incurring a waste of the system resources. On the other hand, including the buffer lengths $\{l_k\}_{k=1}^{K}$ in the relay selection process entails additional $2K\lceil \log_2(L+1) \rceil$ signaling bits. Therefore, the signaling overhead of $2K$ bits needed by the proposed schemes is advantageously smaller than the signaling overheads associated with relaying protocols that include the path gains and/or the buffer lengths in the relay selection process since $2K \ll 2Kn_b$ and $2K < 2K\lceil \log_2(L+1) \rceil$. (ii): Acquiring the exact values of $\{h_{SR_k}, h_{R_kD}\}_{k=1}^{K}$ entails the transmission of pilot packets from the transmitting nodes and the implementation of involved channel estimation procedures at the receiving nodes. In this context, transmitting pilot signals reduces the effective throughput of the network while implementing full channel state information

(CSI) acquisition increases the complexity of the receivers. Moreover, errors in acquiring the exact CSI will translate into performance losses since an inadequate link might be selected and activated.

For implementing the relay selection protocol, one of the network's nodes needs to serve as the cental node where the decision-making policy is applied. For example, the source node S can play the role of the central node. In this context, each one of the K relays shares with the central node 2 signaling bits capturing the availabilities of the relay's links with S and D. The $2K$ signaling bits are collected at the central node and used to construct the sets $\mathcal{C}_t$ and $\mathcal{C}_r$ based on which the relaying schemes are implemented (refer to Algorithm 1 and Algorithm 2). In this context, each relay inspects the content of its buffer to determine whether it is empty or full. Moreover, cyclic redundancy checks (CRC) can be applied on the packets exchanged between the relays and the terminal nodes S and D in order to determine if the corresponding links are in outage or not. Finally, after applying the relay selection procedure, the central node shares two bits with each one of the relays informing this node to transmit, receive, remain idle or concurrently transmit and receive.

III. MARKOV CHAIN FRAMEWORK

A Markov chain (MC) analysis will be adopted for evaluating the performance of the BA cooperative network. A state of the MC corresponds to the numbers of packets stored in the relays' buffers $(l_1,\ldots,l_K) \in \{0,\ldots,L\}^K$ resulting in a total of $N_s \triangleq (L+1)^K$ possible states. The first step in the MC analysis is to derive the transition probabilities $t_{(l_1,\ldots,l_K),(l'_1,\ldots,l'_K)}$ from the state $(l_1,\ldots,l_K)$ to the state $(l'_1,\ldots,l'_K)$ for all states in $\{0,\ldots,L\}^K$. The transition probabilities lead to the steady-state distribution $\{\pi_{(l_1,\ldots,l_K)}\ ;\ (l_1,\ldots,l_K) \in \{0,\ldots,L\}^K\}$ where $\pi_{(l_1,\ldots,l_K)}$ stands for the probability of being in state $(l_1,\ldots,l_K)$ when the MC reaches steady-state. Finally, the steady-state distribution directly yields to the evaluation of the OP and APD.

A. TRANSITION PROBABILITIES

For both of the proposed FD BA schemes, a self transition $(l_1,\ldots,l_K) \rightarrow (l_1,\ldots,l_K)$ occurs in one of the two following cases. (i): All links in the network are unavailable with probability $\prod_{k=1}^{K} p_k q_k$. (ii): At least one of the end-to-end S-R-D links is available where, in this case, the selected relay transmits a packet to D while receiving a packet from S implying no change in the numbers of stored packets. A S-R$_k$-D link is available if both the S-R$_k$ and R$_k$-D links are available with probability $(1-p_k)(1-q_k)$ implying that the unavailability probability of the S-R$_k$-D link is equal to $1-(1-p_k)(1-q_k)$. Therefore, for scheme 1 and scheme 2:

$$t_{(l_1,\ldots,l_K),(l_1,\ldots,l_K)} = \prod_{k=1}^{K} p_k q_k + \left[1 - \prod_{k=1}^{K}[1-(1-p_k)(1-q_k)]\right]. \quad (5)$$

If all end-to-end links are unavailable and the network is not in outage, then a relay out of the K relays is selected to either receive or transmit. Denoting this relay by R$_i$, then the corresponding transition is given by $(l_1,\ldots,l_K) \rightarrow (l'_1,\ldots,l'_K)$ with $l'_k = l_k$ for $k \neq i$ while $l'_i = l_i + 1$ if R$_i$ is selected to receive and $l'_i = l_i - 1$ if R$_i$ is selected to transmit. The transition probabilities in these cases differ between scheme 1 and scheme 2.

1) SCHEME 1

Consider the transition $(l_1,\ldots,l_K) \rightarrow (l_1,\ldots,l_K)+\mathbf{e}_i$ for $i \in \{1,\ldots,K\}$ where $\mathbf{e}_i$ denotes the i-th row of the $K\times K$ identity matrix. In this case, R$_i$ is selected for reception and this transition occurs only when $l_i \neq L$. For the aforementioned transition to occur, the link S-R$_i$ must be available so that a packet can be delivered to R$_i$. Moreover, the link R$_i$-D must be unavailable since, otherwise, both the S-R$_i$ and R$_i$-D links will be available implying that R$_i$ can simultaneously transmit and receive resulting in a self transition as in (5).

Excluding the link R$_i$-D (that should be unavailable), consider the case where the links R$_k$-D are available for all $k \in \mathcal{A}$ for any set $\mathcal{A} \subset \{1,\ldots,K\}\backslash\{i\}$. The probability of this event is $\Pr(\mathcal{A}) = \prod_{k\in\mathcal{A}}[(1-q_k)p_k]\prod_{k'\in\bar{\mathcal{A}}} q_{k'}$ since the links R$_{k'}$-D for $k' \in \bar{\mathcal{A}} \triangleq \{1,\ldots,K\}\backslash\{i\}\backslash\mathcal{A}$ are unavailable. Moreover, the links S-R$_k$ for $k \in \mathcal{A}$ should be unavailable since, otherwise, an end-to-end link will become available resulting in a self transition when the selected relay concurrently transmits and receives. Since the link S-R$_i$ is available and the links S-R$_k$ for $k \in \mathcal{A}$ are unavailable, we denote by $\mathcal{S} \subset \bar{\mathcal{A}}$ the subset of relays in $\bar{\mathcal{A}}$ such that the S-R links are available. In this case, the link S-R$_i$, the links $\{$R$_k$-D ; $k \in \mathcal{A}\}$ and the links $\{$S-R$_j$; $j \in \mathcal{S}\}$ are all available implying that the total number of available links in the network is equal to $|\mathcal{A}|+|\mathcal{S}|+1$. As such, the random selection of the link S-R$_i$ among all available links occurs with probability $\frac{1}{|\mathcal{A}|+|\mathcal{S}|+1}$. Therefore:

$$\begin{aligned} &t_{(l_1,\ldots,l_K),(l_1,\ldots,l_K)+\mathbf{e}_i} \\ &= (1-p_i)q_i \times \sum_{\mathcal{A}\subset\{1,\ldots,K\}\backslash\{i\}} \\ &\quad\times\left[\prod_{k\in\mathcal{A}}[(1-q_k)p_k] \prod_{k'\in\bar{\mathcal{A}}=\{1,\ldots,K\}\backslash\{i\}\backslash\mathcal{A}} q_{k'}\right. \\ &\quad\left.\times \sum_{\mathcal{S}\subset\bar{\mathcal{A}}} \frac{1}{|\mathcal{A}|+|\mathcal{S}|+1}\prod_{j\in\mathcal{S}}(1-p_j)\prod_{j'\in\bar{\mathcal{A}}\backslash\mathcal{S}} p_{j'}\right]; i=1,\ldots,K. \end{aligned} \quad (6)$$

Note that, when $l_i = L$, $p_i = 1$ implying that the probability in (6) will be equal to zero implying that the corresponding transition $(l_1,\ldots,l_K) \rightarrow (l_1,\ldots,l_K)+\mathbf{e}_i$ cannot take place.

Consider now the transition $(l_1,\ldots,l_K) \rightarrow (l_1,\ldots,l_K)-\mathbf{e}_i$ where R$_i$ is selected for transmission. Since scheme 1 does not differentiate between the S-R and R-D links when

performing a random selection between the available links, then the probability of this transition can be obtained by interchanging the roles of the unavailability probabilities p_k and q_k in (6):

$$t_{(l_1,\ldots,l_K),(l_1,\ldots,l_K)-\mathbf{e}_i} = (1-q_i)p_i \times \sum_{\mathcal{A}\subset\{1,\ldots,K\}\setminus\{i\}} \times \left[\prod_{k\in\mathcal{A}}[(1-p_k)q_k] \prod_{k'\in\bar{\mathcal{A}}=\{1,\ldots,K\}\setminus\{i\}\setminus\mathcal{A}} p_{k'} \times \sum_{\mathcal{S}\subset\bar{\mathcal{A}}} \frac{1}{|\mathcal{A}|+|\mathcal{S}|+1} \prod_{j\in\mathcal{S}}(1-q_j) \prod_{j'\in\bar{\mathcal{A}}\setminus\mathcal{S}} q_{j'}\right]; i=1,\ldots,K, \tag{7}$$

where $\mathcal{A}$ and $\mathcal{S}$ now denote the sets of relays possessing available links with S and D, respectively, with $\mathcal{A}\cap\mathcal{S}=\phi$ since otherwise an end-to-end link will be available. Note that $t_{(l_1,\ldots,l_K),(l_1,\ldots,l_K)-\mathbf{e}_i}=0$ when $l_i=0$ since $q_i=1$ in this case following from (4).

2) SCHEME 2

Scheme 2 prioritizes transmission over reception and, as such, a S-R link is activated only when all R-D links are unavailable. Since the set $\mathcal{A}$ in (6) denotes the relays (excluding R_i) with available R-D links, then the transition probability $t_{(l_1,\ldots,l_K),(l_1,\ldots,l_K)+\mathbf{e}_i}$ for scheme 2 can be obtained by setting $\mathcal{A}=\phi$ in (6):

$$t_{(l_1,\ldots,l_K),(l_1,\ldots,l_K)+\mathbf{e}_i} = (1-p_i)\prod_{k=1}^{K} q_k \sum_{\mathcal{S}\subset\{1,\ldots,K\}\setminus\{i\}} \frac{1}{|\mathcal{S}|+1} \times \prod_{j\in\mathcal{S}}(1-p_j) \prod_{j'\in\bar{\mathcal{S}}=\{1,\ldots,K\}\setminus\{i\}\setminus\mathcal{S}} p_{j'}\ ;\ i=1,\ldots,K, \tag{8}$$

where the link S-R_i is available, all R-D links are unavailable and a random selection is made between the $|\mathcal{S}|+1$ relays in $\mathcal{S}\cup\{i\}$.

For the transition $(l_1,\ldots,l_K)\rightarrow(l_1,\ldots,l_K)-\mathbf{e}_i$, the selection is made among the relays in $\mathcal{A}\cup\{i\}$ comprising $|\mathcal{A}|+1$ relays with available R-D links where the available S-R links are not included in the selection since the more prior transmission mode is triggered. Consequently:

$$t_{(l_1,\ldots,l_K),(l_1,\ldots,l_K)-\mathbf{e}_i} = (1-q_i)p_i \sum_{\mathcal{A}\subset\{1,\ldots,K\}\setminus\{i\}} \frac{1}{|\mathcal{A}|+1} \times \prod_{k\in\mathcal{A}}[(1-q_k)p_k] \prod_{k'\in\bar{\mathcal{A}}=\{1,\ldots,K\}\setminus\{i\}\setminus\mathcal{A}} q_{k'}\ ;\ i=1,\ldots,K. \tag{9}$$

B. STEADY-STATE DISTRIBUTION, OP AND APD

Consider the set $\mathcal{D}$ of cardinality $2K+1$ given by $\mathcal{D}=\{(0,\ldots,0)\}\cup\{\pm e_i\ ;\ i=1,\ldots,K\}$. The transition probabilities satisfy the relation $\sum_{\mathbf{d}\in\mathcal{D}} t_{(l_1,\ldots,l_K),(l_1,\ldots,l_K)+\mathbf{d}}=1$ for all $(l_1,\ldots,l_K)\in\{0,\ldots,L\}^K$. The balance equation at state $(l_1,\ldots,l_K)$ is given by:

$$\pi_{(l_1,\ldots,l_K)} = \sum_{\mathbf{d}\in\mathcal{D}} t_{(l_1,\ldots,l_K)+\mathbf{d},(l_1,\ldots,l_K)}\pi_{(l_1,\ldots,l_K)+\mathbf{d}} \quad \forall\ (l_1,\ldots,l_K)\in\{0,\ldots,L\}^K. \tag{10}$$

The steady-state distribution can be obtained by solving any N_s-1 equations out of the N_s equations in (10) along with the equation $\sum_{(l_1,\ldots,l_K)\in\{0,\ldots,L\}^K}\pi_{(l_1,\ldots,l_K)}=1$. This procedure is equivalent to the relation [3]:

$$\pi = (\mathbf{T}-\mathbf{I}+\mathbf{B})^{-1}\mathbf{b}, \tag{11}$$

where π and $\mathbf{T}$ are $N_s\times 1$ and $N_s\times N_s$ matrices stacking the steady-state probabilities and transition probabilities, respectively. $\mathbf{I}$ and $\mathbf{B}$ are the $N_s\times N_s$ matrices denoting the identity matrix and the all-one matrix, respectively. $\mathbf{b}$ is the vector whose elements are all equal to 1.

The steady-state distribution is useful for evaluating the OP and APD. The cooperative network is said to be in outage when no packets can be communicated along any of its constituent links following from the unavailability of these links. As such, the OP can be derived from [5]:

$$OP = \sum_{l_1=0}^{L}\cdots\sum_{l_K=0}^{L}\pi_{(l_1,\ldots,l_K)}\left[\prod_{k=1}^{K}p_k q_k\right], \tag{12}$$

where the unavailability probabilities $\{p_k, q_k\}$ depend on the buffer length l_k according to (3)-(4).

The storage of the packets in the relays' buffers incurs delays in the delivery of the packets to D. Following from [16], the APD can be determined from:

$$APD = \frac{\bar{L}+1}{\eta_s} - 1, \tag{13}$$

where $\bar{L}$ denotes the average queue length:

$$\bar{L} = \sum_{l_1=0}^{L}\cdots\sum_{l_K=0}^{L}\pi_{(l_1,\ldots,l_K)}\left[\sum_{k=1}^{K} l_k\right], \tag{14}$$

while η_s stands for the input throughput at the relays:

$$\eta_s = \sum_{l_1=0}^{L}\cdots\sum_{l_K=0}^{L}\pi_{(l_1,\ldots,l_K)}\left[1-\prod_{k=1}^{K}p_k\right]. \tag{15}$$

IV. ASYMPTOTIC PERFORMANCE ANALYSIS

An exact MC analysis that accounts for all $(L+1)^K$ states is out of reach especially for large values of K and/or L where the number of states becomes prohibitively large rendering the solution of all balance equations in (10) intractable. Since the fading-mitigation cooperative techniques result in the highest performance gains at high SNRs, we adopt the high-SNR assumption as in [3], [4], and [5]. For asymptotically large values of the SNR, the transition

probabilities between some states can be ignored and the analysis can focus on a small set of states that dominate the asymptotic performance. This approach results in a tractable analysis and in simple closed-form expressions of the OP and APD that are useful for offering intuitive insights on the system performance without sacrificing the accuracy at high SNRs.

The asymptotic analysis revolves around the identification of a subset of states that is closed at high SNRs. A subset of states $\mathcal{C}$ is said to be closed if the probability of exiting this subset tends to zero:

$$t_{(l_1,\ldots,l_K),(l'_1,\ldots,l'_K)} \to 0 \; \forall \; (l_1,\ldots,l_K) \in \mathcal{C} \; \& \; (l'_1,\ldots,l'_K) \notin \mathcal{C}. \tag{16}$$

The implications of (16) are as follows. After a certain number of transitions, the MC will move to the closed-subset $\mathcal{C}$ and remain in this subset at steady-state. As such, when the MC reaches equilibrium, the total steady-state probability of one will be divided among elements of $\mathcal{C}$ and the steady-state probabilities of states outside $\mathcal{C}$ will tend to zero asymptotically since exiting $\mathcal{C}$ is highly improbable. Therefore, the asymptotic analysis focuses on elements of $\mathcal{C}$ in an attempt to simplify the analysis and reach tractable results with high level of accuracy at high SNR. Following from (12), the asymptotic value of the OP can be determined from:

$$OP = \sum_{(l_1,\ldots,l_K)\in\mathcal{C}} \pi_{(l_1,\ldots,l_K)} \left[\prod_{k=1}^{K} p_k q_k\right]. \tag{17}$$

Similarly, the input throughput in (15) tends to 1 asymptotically implying, from (13) and (14), that the APD tends to the following value at high SNRs:

$$APD = \bar{L} = \sum_{(l_1,\ldots,l_K)\in\mathcal{C}} \pi_{(l_1,\ldots,l_K)} \left[\sum_{k=1}^{K} l_k\right]. \tag{18}$$

For the sake of simplicity, we consider the case of a quasi-symmetrical network where the distances and fading conditions between S and the relays, on one hand, and between the relays and D, on the other hand, are the same. In other words, we assume that $\mathfrak{p}_1 = \cdots = \mathfrak{p}_K \triangleq \mathfrak{p}$ and $\mathfrak{q}_1 = \cdots = \mathfrak{q}_K \triangleq \mathfrak{q}$.

A. SPECIAL CASE: K = 2 RELAYS

In order to offer clear insights on the calculation methodology, we first tackle the special case of two relays then extend the analysis to the more challenging case of an arbitrary number of relays in the next subsection.

1) SCHEME 1

Replacing $K = 2$ in (5), (6) and (7) results in:

$$t_{(l_1,l_2),(l_1,l_2)} = p_1p_2q_1q_2 + 1 - (p_1 + q_1 - p_1q_1)(p_2 + q_2 - p_2q_2) \tag{19}$$

$$t_{(l_1,l_2),(l_1,l_2)+\mathbf{e}_i} = (1-p_i)q_i \times \left[p_{\bar{i}}q_{\bar{i}} + \frac{1}{2}(1-p_{\bar{i}})q_{\bar{i}} + \frac{1}{2}(1-q_{\bar{i}})p_{\bar{i}}\right]; \; i = 1, 2 \tag{20}$$

$$t_{(l_1,l_2),(l_1,l_2)-\mathbf{e}_i} = (1-q_i)p_i \times \left[p_{\bar{i}}q_{\bar{i}} + \frac{1}{2}(1-q_{\bar{i}})p_{\bar{i}} + \frac{1}{2}(1-p_{\bar{i}})q_{\bar{i}}\right]; \; i = 1, 2, \tag{21}$$

where $\bar{i} = 2$ if $i = 1$ and $\bar{i} = 1$ if $i = 2$.

Note that the S-R (resp. R-D) unavailability probabilities p_1 and p_2 (resp. q_1 and q_2) might not be the same even though the outage probabilities satisfy $\mathfrak{p}_1 = \mathfrak{p}_2$ (resp. $\mathfrak{q}_1 = \mathfrak{q}_2$). This follows since the unavailability probabilities depend on the buffers' lengths based on (3)-(4).

Equations (19)-(21) can be used to construct the state diagram shown in Fig. 1 where the high order probabilities are ignored at high SNR. For example, consider the state $(0, l)$ for $l \neq 0, L$. For this state, $q_1 = 1$ while $p_1 = p_2 = \mathfrak{p}$ and $q_2 = \mathfrak{q}$. Replacing in (19) results in $t_{(0,l),(0,l)} = \mathfrak{p}^2\mathfrak{q} + 1 - (\mathfrak{p} + \mathfrak{q} - \mathfrak{p}\mathfrak{q}) \approx 1 - \mathfrak{p} - \mathfrak{q}$ since the probabilities $\mathfrak{p}^2\mathfrak{q}$ and $\mathfrak{p}\mathfrak{q}$ can be neglected compared to the outage probabilities $\mathfrak{p}$ and $\mathfrak{q}$ when $\mathfrak{p} \ll 1$ and $\mathfrak{q} \ll 1$ at high SNR. Replacing $i = 1$ and $i = 2$ in (20) results in $t_{(0,l),(1,l)} = (1-\mathfrak{p})\frac{(\mathfrak{p}+\mathfrak{q})}{2} \approx \frac{\mathfrak{p}+\mathfrak{q}}{2}$ and $t_{(0,l),(0,l+1)} = (1-\mathfrak{p})\mathfrak{q}\frac{1+\mathfrak{p}}{2} \approx \frac{\mathfrak{q}}{2}$, respectively. Finally, setting $i = 2$ in (21) results in $t_{(0,l),(0,l-1)} = (1-\mathfrak{q})\mathfrak{p}\frac{1+\mathfrak{p}}{2} \approx \frac{\mathfrak{p}}{2}$ while the transition associated with $i = 1$ is infeasible since R_1 cannot transmit (the corresponding transition probability is zero). A similar approximation approach is applied at the remaining states to construct the state diagram in Fig. 1.

Consider the case $\mathfrak{q} \ll \mathfrak{p}$ where the relays are closer to D. In this case, it can be observed from Fig. 1 that the closed-subset is given by $\mathcal{C} = \{(0,0), (0,1), (1,0), (1,1)\}$. From Fig. 1, four transitions can lead outside $\mathcal{C}$; namely, the transitions $(0,1) \to (0,2)$, $(1,0) \to (2,0)$, $(1,1) \to (1,2)$ and $(1,1) \to (2,1)$. However, these transitions occur with probabilities $t_{(0,1),(0,2)} = t_{(1,0),(2,0)} = \frac{\mathfrak{q}}{2}$ and $t_{(1,1),(1,2)} = t_{(1,1),(2,1)} = \frac{\mathfrak{q}(\mathfrak{p}+\mathfrak{q})}{2}$ where these probabilities tends to zero asymptotically since $\mathfrak{q} \ll 1$ in the considered case. Ignoring the probability $\mathfrak{q}$ compared to $\mathfrak{p}$, the balance equations at elements of $\mathcal{C}$ are given by: $\mathfrak{p}^2\pi_{(1,1)} = \frac{\mathfrak{p}}{2}\pi_{(0,1)} + \frac{\mathfrak{p}}{2}\pi_{(1,0)}$, $\mathfrak{p}\pi_{(0,1)} = \frac{1}{2}\pi_{(0,0)} + \frac{\mathfrak{p}^2}{2}\pi_{(1,1)}$, $\mathfrak{p}\pi_{(1,0)} = \frac{1}{2}\pi_{(0,0)} + \frac{\mathfrak{p}^2}{2}\pi_{(1,1)}$ and $\pi_{(0,0)} = \frac{\mathfrak{p}}{2}\pi_{(0,1)} + \frac{\mathfrak{p}}{2}\pi_{(1,0)}$. Solving three of these equations along with the relation $\pi_{(0,0)} + \pi_{(0,1)} + \pi_{(1,0)} + \pi_{(1,1)} \to 1$ results in the following asymptotic values of the steady-state probabilities at elements of $\mathcal{C}$:

$$\begin{aligned}
\pi_{(0,0)} &= \frac{\mathfrak{p}^2}{(1+\mathfrak{p})^2} \approx \mathfrak{p}^2 \\
\pi_{(0,1)} = \pi_{(1,0)} &= \frac{\mathfrak{p}}{(1+\mathfrak{p})^2} \approx \mathfrak{p} \\
\pi_{(1,1)} &= \frac{1}{(1+\mathfrak{p})^2} \approx 1 - 2\mathfrak{p} - \mathfrak{p}^2.
\end{aligned} \tag{22}$$

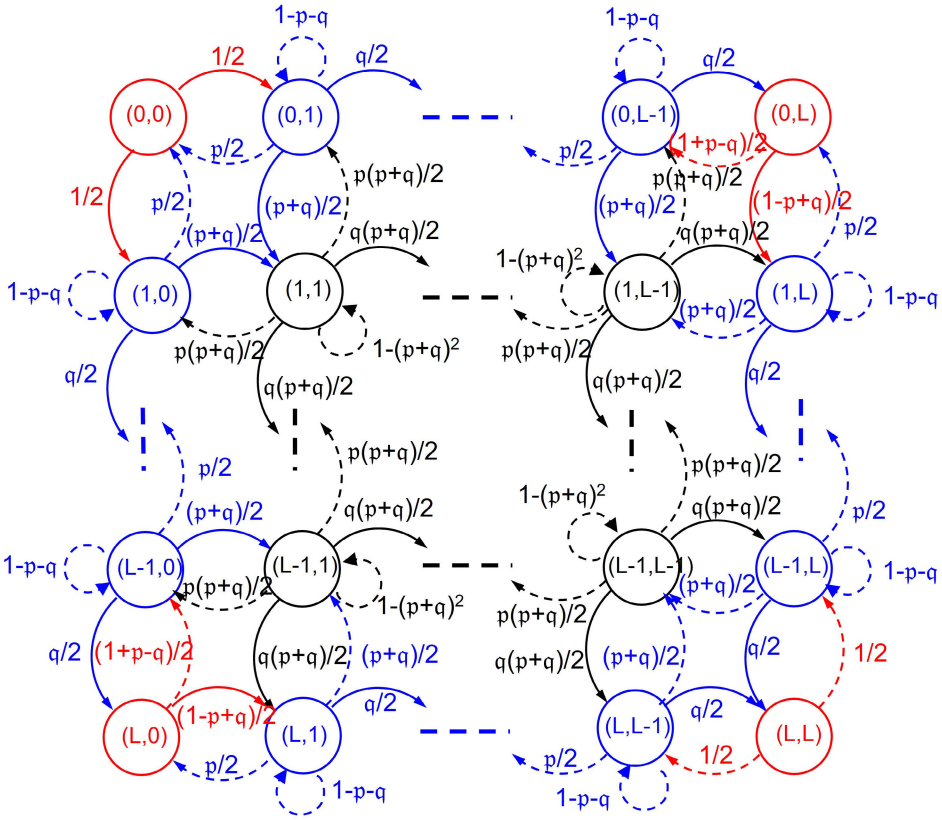

FIGURE 1. State diagram of scheme 1 with $K = 2$.

Replacing (22) in (17) results in the following asymptotic expression of the OP:

$$\begin{aligned} OP &= \pi_{(0,0)}\mathfrak{p}^2 + \pi_{(0,1)}\mathfrak{p}^2\mathfrak{q} + \pi_{(1,0)}\mathfrak{p}^2\mathfrak{q} + \pi_{(1,1)}\mathfrak{p}^2\mathfrak{q}^2 \\ &= \frac{\mathfrak{p}^2}{(1+\mathfrak{p})^2}[\mathfrak{p}^2 + 2\mathfrak{p}\mathfrak{q} + \mathfrak{q}^2] = \frac{\mathfrak{p}^2}{(1+\mathfrak{p})^2}(\mathfrak{p}+\mathfrak{q})^2 \\ &\approx \mathfrak{p}^4 = \max\{\mathfrak{p},\mathfrak{q}\}^4, \end{aligned} \tag{23}$$

since $l_k = 0 \Rightarrow q_k = 1$, $l_k \neq 0 \Rightarrow q_k = \mathfrak{q}_k = \mathfrak{q}$, $l_k = L \Rightarrow p_k = 1$, $l_k \neq L \Rightarrow p_k = \mathfrak{p}_k = \mathfrak{p}$ for $k = 1, 2$ following from (3)-(4).

From (18) and (22), the asymptotic APD is given by:

$$APD = \frac{1}{(1+\mathfrak{p}^2)}\left[2\mathfrak{p} + 2(1-2\mathfrak{p}-\mathfrak{p}^2)\right] \approx 2. \tag{24}$$

Consider now the case $\mathfrak{p} \ll \mathfrak{q}$ where the relays are closer to S. From Fig. 1, it can be observed that $\mathcal{C} = \{(L,L), (L-1,L), (L,L-1), (L-1,L-1)\}$ forms a closed-subset. In fact, the transition probabilities from elements of $\mathcal{C}$ to elements outside $\mathcal{C}$ are given by $\pi_{(L-1,L),(L-2,L)} = \pi_{(L,L-1),(L,L-2)} = \frac{\mathfrak{p}}{2}$ and $\pi_{(L-1,L-1),(L-2,L-1)} = \pi_{(L-1,L-1),(L-1,L-2)} = \frac{\mathfrak{p}(\mathfrak{p}+\mathfrak{q})}{2}$ where these probabilities tend to zero for $\mathfrak{p} \ll 1$. From Fig. 1, it can be observed that the transition probabilities among the elements of $\mathcal{C}$ in the case $\mathfrak{p} \ll \mathfrak{q}$ can be obtained from those in the case $\mathfrak{q} \ll \mathfrak{p}$ by interchanging the roles of the outage probabilities $\mathfrak{p}$ and $\mathfrak{q}$. Therefore, from (22), the steady-state probabilities of elements of $\mathcal{C}$ when $\mathfrak{p} \ll \mathfrak{q}$ are given by:

$$\begin{aligned} &\pi_{(L,L)} \to \mathfrak{q}^2 \\ &\pi_{(L-1,L)} = \pi_{(L,L-1)} \to \mathfrak{q} \\ &\pi_{(L-1,L-1)} \to 1 - 2\mathfrak{q} - \mathfrak{q}^2. \end{aligned} \tag{25}$$

Replacing (25) in (17) and (18) results in:

$$OP \approx \mathfrak{q}^4 = \max\{\mathfrak{p},\mathfrak{q}\}^4 \tag{26}$$

$$APD \approx 2(L-1). \tag{27}$$

Note that, in the case $\mathfrak{p} \ll \mathfrak{q}$, the quality of the R-D links is significantly inferior to that of the S-R links. As such, the R-D links will regularly suffer from outage with high probability implying that the relays will often operate in the reception mode. Therefore, the numbers of received packets that will eventually stored in the relays' buffers will consistently increase until they reach the value of L. This behaviour of the network is reflected in (25) that shows that the probability of having full buffers is nonzero. In fact, the buffer at R_1 is full with probability $\pi_{(L,L-1)} + \pi_{(L,L)} \to \mathfrak{q} + \mathfrak{q}^2 \neq 0$. Similarly, the buffer at R_2 is full with probability $\pi_{(L-1,L)} + \pi_{(L,L)} \to \mathfrak{q} + \mathfrak{q}^2 \neq 0$.

2) SCHEME 2

Since both scheme 1 and scheme 2 prioritize the activation of an available end-to-end link, then the probability of

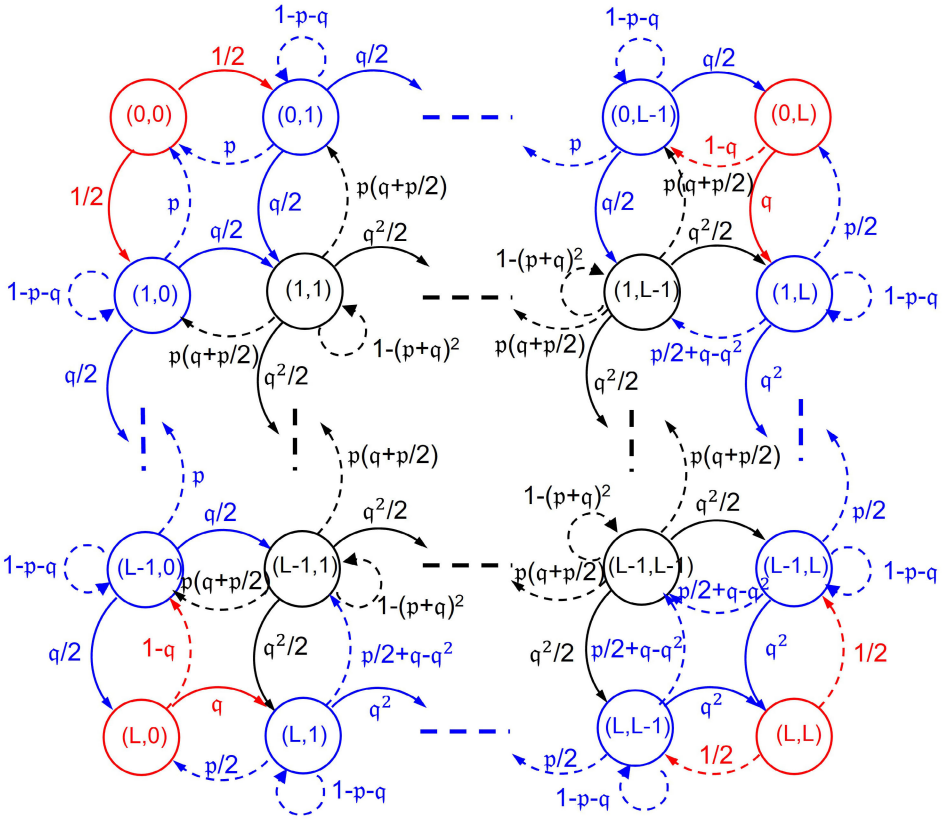

FIGURE 2. State diagram of scheme 2 with $K = 2$.

self-transition for scheme 2 is as given in (19). Replacing $K = 2$ in (8) and (9) results in:

$$t_{(l_1,l_2),(l_1,l_2)+\mathbf{e}_i} = (1-p_i)q_1q_2\left[p_{\bar{i}} + \frac{1}{2}(1-p_{\bar{i}})\right]\ ;\ i = 1,2 \tag{28}$$

$$t_{(l_1,l_2),(l_1,l_2)-\mathbf{e}_i} = (1-q_i)p_i\left[q_{\bar{i}} + \frac{1}{2}(1-q_{\bar{i}})p_{\bar{i}}\right]\ ;\ i = 1,2. \tag{29}$$

Ignoring the high order probabilities at high SNR, the state diagram of scheme 2 is as shown in Fig. 2. For $\mathfrak{q} \ll \mathfrak{p}$, the closed-subset is given by $\mathcal{C} = \{(0,0),(0,1),(1,0),(1,1)\}$ as in the case of scheme 1. From Fig. 2, the probabilities of the transitions that yield out of $\mathcal{C}$ are given by $t_{(0,1),(0,2)} = t_{(1,0),(2,0)} = \frac{\mathfrak{q}}{2}$ and $t_{(1,1),(1,2)} = t_{(1,1),(2,1)} = \frac{\mathfrak{q}^2}{2}$ where these probabilities tend to zero when $\mathfrak{q} \ll 1$ implying that $\mathcal{C}$ is closed asymptotically. The balance equation at the state $(1,1)$ implies that $\pi_{(1,1)} = 0$ since there are no transitions entering this state from other elements of $\mathcal{C}$ when $\mathfrak{q} \ll 1$. The balance equations at states $(0,1)$ and $(1,0)$ imply that $\mathfrak{p}\pi_{(0,1)} = \mathfrak{p}\pi_{(1,0)} = \frac{1}{2}\pi_{(0,0)}$. Replacing these relations in the equation $\pi_{(0,0)} + \pi_{(0,1)} + \pi_{(1,0)} = 1$ implies that:

$$\pi_{(0,0)} = \frac{\mathfrak{p}}{1+\mathfrak{p}} \approx \mathfrak{p}$$

$$\pi_{(0,1)} = \pi_{(1,0)} = \frac{1}{2(1+\mathfrak{p})} \approx \frac{1-\mathfrak{p}}{2}$$

$$\pi_{(1,1)} \to 0. \tag{30}$$

Replacing (30) in (17) and (18) results in:

$$OP = \mathfrak{p}(\mathfrak{p}^2) + 2 \times \frac{1-\mathfrak{p}}{2}(\mathfrak{p}^2\mathfrak{q}) = \mathfrak{p}^2(\mathfrak{p}+\mathfrak{q}) \approx \mathfrak{p}^3 = \max\{\mathfrak{p},\mathfrak{q}\}^3 \tag{31}$$

$$APD = 2 \times \frac{1-\mathfrak{p}}{2} \times 1 = 1-\mathfrak{p} \approx 1. \tag{32}$$

As with scheme 1, the subset $\mathcal{C} = \{(L,L),(L-1,L),(L,L-1),(L-1,L-1)\}$ is closed in the case $\mathfrak{p} \ll \mathfrak{q}$ since, from Fig. 2, $t_{(L-1,L),(L-2,L)} = t_{(L,L-1),(L,L-2)} = \frac{\mathfrak{p}}{2} \to 0$ and $t_{(L-1,L-1),(L-2,L-1)} = t_{(L-1,L-1),(L-1,L-2)} = \frac{\mathfrak{p}^2}{2} \to 0$ when $\mathfrak{p} \to 0$. Solving for the steady-state distribution of the elements of $\mathcal{C}$ results in:

$$\pi_{(L,L)} \to \mathfrak{q}^3$$

$$\pi_{(L-1,L)} = \pi_{(L,L-1)} \to \frac{\mathfrak{q}}{2}$$

$$\pi_{(L-1,L-1)} \to 1-\mathfrak{q}-\mathfrak{q}^3 \approx 1-\mathfrak{q}. \tag{33}$$

Replacing (33) in (17) and (18) results in (for $\mathfrak{p} \ll \mathfrak{q}$):

$$OP = \mathfrak{q}^3(\mathfrak{q}^2) + 2 \times \frac{\mathfrak{q}}{2}(\mathfrak{p}\mathfrak{q}^2) + (1-\mathfrak{q})(\mathfrak{p}^2\mathfrak{q}^2) \approx \mathfrak{q}^5 = \max\{\mathfrak{p},\mathfrak{q}\}^5 \tag{34}$$

$$APD = 2 \times \frac{\mathfrak{q}}{2} \times (2L-1) + (1-\mathfrak{q}) \times (2(L-1)) \approx 2(L-1). \tag{35}$$

B. GENERAL CASE: ANY NUMBER OF RELAYS

1) SCHEME 1

Proposition 1: For a cooperative network with K relays, the closed-subset associated with scheme 1 comprises the 2^K states given by:

$$\mathcal{C} = \begin{cases} \{0,1\}^K, & \mathfrak{q} < \mathfrak{p}; \\ \{L-1, L\}^K, & \mathfrak{p} < \mathfrak{q}. \end{cases} \tag{36}$$

where the steady-state probabilities of elements of $\mathcal{C}$ are given by:

$$\pi_{(l_1,\ldots,l_K)} = \begin{cases} \mathfrak{p}^{\chi}(1-\mathfrak{p})^{K-\chi}, & \mathfrak{q} < \mathfrak{p}; \\ \mathfrak{q}^{\psi}(1-\mathfrak{q})^{K-\psi}, & \mathfrak{p} < \mathfrak{q}. \end{cases} \tag{37}$$

where $\chi \triangleq \sum_{k=1}^{K} \delta_{l_k=0}$ and $\psi \triangleq \sum_{k=1}^{K} \delta_{l_k=L}$ stand for the number of components of the state $(l_1, \ldots, l_K)$ that are equal to 0 and L, respectively.

Proof: The proof is provided in Appendix A. ■

For $\mathfrak{q} < \mathfrak{p}$, replacing (37) in (17) results in $OP = \sum_{\chi=0}^{K} \binom{K}{\chi} \mathfrak{p}^{\chi}(1-\mathfrak{p})^{K-\chi}[\mathfrak{p}^K \mathfrak{q}^{K-\chi}]$ since χ R-D links are unavailable because the corresponding relays' buffers are empty. Since $1-\mathfrak{p} \approx 1$ asymptotically, the above relation can be written as $OP = \mathfrak{p}^K \sum_{\chi=0}^{K} \binom{K}{\chi} \mathfrak{p}^{\chi} \mathfrak{q}^{K-\chi} = \mathfrak{p}^K(\mathfrak{p}+\mathfrak{q})^K \approx \mathfrak{p}^{2K}$ assuming that $\mathfrak{q} \ll \mathfrak{p}$. Similarly, for $\mathfrak{p} < \mathfrak{q}$, replacing (37) in (17) results in $OP = \sum_{\psi=0}^{K} \binom{K}{\psi} \mathfrak{q}^{\psi}(1-\mathfrak{q})^{K-\psi}[\mathfrak{p}^{K-\psi}\mathfrak{q}^K]$ since ψ S-R links are unavailable since ψ components of $(l_1, \ldots, l_K)$ are equal to L (full buffers). The above relation can be further approximated by $OP = \mathfrak{q}^K(\mathfrak{p}+\mathfrak{q})^K \approx \mathfrak{q}^{2K}$ for $\mathfrak{p} \ll \mathfrak{q}$. Therefore, the asymptotic OP of scheme 1 can be written as:

$$OP = \max\{\mathfrak{p}, \mathfrak{q}\}^{2K}. \tag{38}$$

From (18) and (37), the asymptotic APD in the case $\mathfrak{q} < \mathfrak{p}$ can be written as $APD = \sum_{\chi=0}^{K} \binom{K}{\chi} \mathfrak{p}^{\chi}(1-\mathfrak{p})^{K-\chi}[K-\chi]$ since $\sum_{k=1}^{K} l_k = \chi \times 0 + (K-\chi) \times 1 = K - \chi$. Since $\mathfrak{p} \ll 1$ asymptotically, the most dominant term in the APD corresponds to $\chi = 0$ resulting in $APD \to K$. Similarly, for $\mathfrak{p} < \mathfrak{q}$, $APD = \sum_{\psi=0}^{K} \binom{K}{\psi} \mathfrak{q}^{\psi}(1-\mathfrak{q})^{K-\psi}[K(L-1)+\psi]$ since $\sum_{k=1}^{K} l_k = \psi \times L + (K-\psi) \times (L-1) = K(L-1) + \psi$. Because of the term $\mathfrak{q}^{\psi}$, the term corresponding to $\psi = 0$ in the APD is several orders of magnitude larger than the terms corresponding to $\psi \neq 0$ resulting in $APD \to K(L-1)$. Therefore, for scheme 1:

$$APD = \begin{cases} K, & \mathfrak{q} < \mathfrak{p}; \\ K(L-1), & \mathfrak{p} < \mathfrak{q}. \end{cases} \tag{39}$$

2) SCHEME 2

Proposition 2: For scheme 2 with $\mathfrak{q} < \mathfrak{p}$, the closed-subset is given by:

$$\mathcal{C} = \{(0, \ldots, 0)\} \cup \{\mathbf{e}_k \; ; \; k = 1, \ldots, K\}, \tag{40}$$

where the steady-state probabilities of the $K+1$ elements of $\mathcal{C}$ are given by:

$$\begin{cases} \pi_{(0,\ldots,0)} = \mathfrak{p} \\ \pi_{\mathbf{e}_k} = \dfrac{1}{K}(1-\mathfrak{p}) \; ; \; k = 1, \ldots, K. \end{cases} \tag{41}$$

Proof: The proof is provided in Appendix B. ■

Replacing (41) in (17) results in:

$$\begin{aligned} OP &= \mathfrak{p}[\mathfrak{p}^K] + K\frac{1-\mathfrak{p}}{K}[\mathfrak{p}^K \mathfrak{q}] \\ &\approx \mathfrak{p}^K(\mathfrak{p}+\mathfrak{q}) \approx \mathfrak{p}^{K+1} = \max\{\mathfrak{p}, \mathfrak{q}\}^{K+1} \; ; \; \mathfrak{q} < \mathfrak{p}. \end{aligned} \tag{42}$$

Replacing (41) in (18) implies that the asymptotic APD can be determined from:

$$APD = \mathfrak{p} \times 0 + K\frac{1-\mathfrak{p}}{K} \times 1 = 1 \; ; \; \mathfrak{q} < \mathfrak{p}. \tag{43}$$

Proposition 3: For scheme 2 with $\mathfrak{p} < \mathfrak{q}$, the closed-subset is given by:

$$\mathcal{C} = \{L-1, L\}^K, \tag{44}$$

where the steady-state probabilities of the 2^K elements of $\mathcal{C}$ are given by:

$$\pi_{(l_1,\ldots,l_K)} = \begin{cases} 1 - \displaystyle\sum_{k=1}^{K} \mathfrak{q}^{\frac{k(k+1)}{2}} \approx 1, & \psi = 0; \\ \dfrac{1}{\binom{K}{\psi}} \mathfrak{q}^{\frac{\psi(\psi+1)}{2}}, & \psi \neq 0. \end{cases}, \tag{45}$$

where, as in (37), ψ stands for the number of components of $(l_1, \ldots, l_K)$ that are equal to L.

Proof: The proof is provided in Appendix C. ■

Replacing (45) in (17) results in:

$$OP = \mathfrak{p}^K \mathfrak{q}^K + \sum_{\psi=1}^{K} \mathfrak{q}^{\frac{\psi(\psi+1)}{2}} [\mathfrak{p}^{K-\psi}\mathfrak{q}^K], \tag{46}$$

since, for the $\binom{K}{\psi}$ states comprising ψ components that are equal to L, ψ S-R links are unavailable because of the ψ full buffers. For $\mathfrak{p} \ll \mathfrak{q}$, the largest term in the summation in (46) corresponds to $\psi = K$ resulting in:

$$\begin{aligned} OP &= \mathfrak{p}^K \mathfrak{q}^K + \mathfrak{q}^{\frac{K(K+3)}{2}} \approx \mathfrak{q}^{\frac{K(K+3)}{2}} \\ &= \max\{\mathfrak{p}, \mathfrak{q}\}^{\frac{K(K+3)}{2}} \quad \mathfrak{p} < \mathfrak{q}. \end{aligned} \tag{47}$$

Replacing (45) in (18) results in:

$$\begin{aligned} APD &= K(L-1) + \sum_{\psi=1}^{K} \mathfrak{q}^{\frac{\psi(\psi+1)}{2}} [\psi L + (K-\psi)(L-1)] \\ &\approx K(L-1) \;\; \mathfrak{p} < \mathfrak{q}. \end{aligned} \tag{48}$$

TABLE 1. Asymptotic OP and APD values of scheme 1 and scheme 2.

	Scheme 1	Scheme 2
OP	$\max\{\mathfrak{p},\mathfrak{q}\}^{2K}$	$\begin{cases}\max\{\mathfrak{p},\mathfrak{q}\}^{K+1}, & \mathfrak{q}<\mathfrak{p};\\ \max\{\mathfrak{p},\mathfrak{q}\}^{\frac{K(K+3)}{2}}, & \mathfrak{p}<\mathfrak{q}.\end{cases}$
APD	$\begin{cases}K, & \mathfrak{q}<\mathfrak{p};\\ K(L-1), & \mathfrak{p}<\mathfrak{q}.\end{cases}$	$\begin{cases}1, & \mathfrak{q}<\mathfrak{p};\\ K(L-1), & \mathfrak{p}<\mathfrak{q}.\end{cases}$

C. COMPARING SCHEME 1 AND SCHEME 2

For convenience, Table 1 summarizes the asymptotic OP and APD expressions of scheme 1 in (38)- (39) and of scheme 2 in (42)- (43) and (47)-(48). These expressions simplify to the values provided in (23)-(24), (26)-(27), (31)-(32) and (34)-(35) in the special case $K = 2$.

The following conclusions can be drawn from Table 1:

- For $K > 1$, $K+1 < 2K < \frac{K(K+3)}{2}$ which implies the following. (i): For $\mathfrak{q} < \mathfrak{p}$, scheme 1 achieves smaller OP values compared to scheme 2 at the expense of an increased delay. For this scenario, scheme 2 is particularly interesting because of its capability of achieving a very small asymptotic APD value of 1 regardless of the number of relays. This highlights on the importance of FD BA relaying since none of the existing HD BA relaying schemes can achieve an APD below 2. (ii): For $\mathfrak{p} < \mathfrak{q}$, scheme 2 outperforms scheme 1 in terms of the OP with the same asymptotic APD value rendering the former scheme more adequate to this scenario. In fact, when $\mathfrak{p} < \mathfrak{q}$, the relays' buffers are more congested since the S-R links are stronger than the R-D links implying that the arrival rate exceeds the departure rate causing the APD to increase with the buffer size L. As such, scheme 2 that prioritizes the transmission results in emptying the buffers at a faster pace making this scheme an adequate option for increasing the departure rate to balance the high arrival rate.
- For $K = 1$, $K+1 = 2K = \frac{K(K+3)}{2}$ implying that both schemes achieve the same OP and APD values. In this case, both schemes are equivalent. In fact, when the S-R and R-D links are available, the FD relay simultaneously transmits and receives with both schemes. Otherwise, either both links are unavailable and the system is in outage or only one link is available implying that this link will be activated with both schemes.
- The asymptotic OPs of both schemes do not depend on L implying that there is no benefit in increasing L beyond 2. In fact, L cannot be equal to 1 since the buffers will be either full or empty all the time which severely penalizes the performance. When $\mathfrak{q} < \mathfrak{p}$, the asymptotic APD does not depend on L since in this case the arrival rate is small and rarely a packet fills a position beyond the second slot in the buffer for large SNRs. On the other hand, the asymptotic APD depends on L when $\mathfrak{p} < \mathfrak{q}$ since the arrival rate is high. In this case, fixing $L = 2$ minimizes the asymptotic delay to $APD = K$ without penalizing the OP.

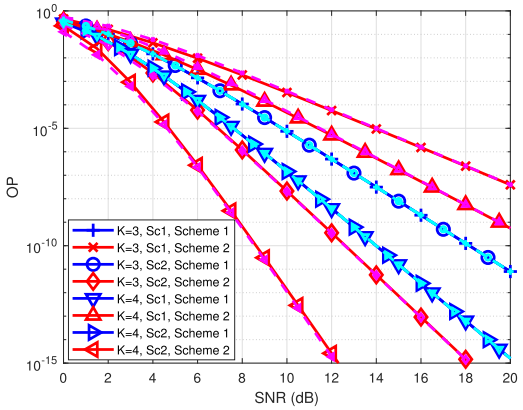

FIGURE 3. OP performance with $L = 4$. $(d_{SR}, d_{RD}) = (4, 2)$ km and $(d_{SR}, d_{RD}) = (2, 4)$ km in scenario 1 (Sc1) and scenario 2 (Sc2), respectively. Solid and dashes lines correspond to the exact and asymptotic values, respectively.

V. NUMERICAL RESULTS

We assume that S and D are separated by 5 km and we assume a path loss exponent of 2. We consider the cases where the S-R and R-D distances are fixed to 2 km, 3 km or 4 km for which the parameters of the $\kappa - \mu$ distribution are fixed to $(\kappa, \mu, \Omega) = (1.5, 3, (5/2)^2)$, $(\kappa, \mu, \Omega) = (1.25, 2, (5/3)^2)$ and $(\kappa, \mu, \Omega) = (1, 1, (5/4)^2)$, respectively. We assume that all relays are placed at a distance d_{SR} from S and d_{RD} from D. Finally, we fix $r_0 = 1$ BPCU. In figures 3-8, we assume perfect SI cancellation (i.e. $\beta = 0$) while the impact of residual SI is investigated in figures 9-12.

Fig. 3 and Fig. 4 show the OP and APD performances, respectively, with $K = 3$ and $K = 4$ for a buffer size of $L = 4$. We consider the two following scenarios. In scenario 1, the relays are placed closer to D with $(d_{SR}, d_{RD}) = (4, 2)$ km resulting in $\mathfrak{q} < \mathfrak{p}$. In scenario 2, the relays are placed closer to S with $(d_{SR}, d_{RD}) = (2, 4)$ km resulting in $\mathfrak{p} < \mathfrak{q}$. In order to validate the accuracy of the presented asymptotic analysis, we plot the exact results as well as the asymptotic OP and APD values reported in Table 1. Results in Fig. 3 show that the derived OP expressions yield extremely accurate results for average-to-large values of the SNR. These results demonstrate that scheme 1 achieves the same OP performance in both scenarios which is coherent with the derived asymptotic OP expression of $\max\{\mathfrak{p}, \mathfrak{q}\}^{2K}$ that holds whether $\mathfrak{q} < \mathfrak{p}$ or $\mathfrak{p} < \mathfrak{q}$. This OP behaviour of scheme 1 differs from that of scheme 2 that yields the highest OP gains in scenario 2 in coherence with Table 1. Finally, results in Fig. 3 highlight on the enhanced diversity gains that can be reaped by increasing the number of relays. Fig. 4 demonstrates that the APD curves converge to the asymptotic

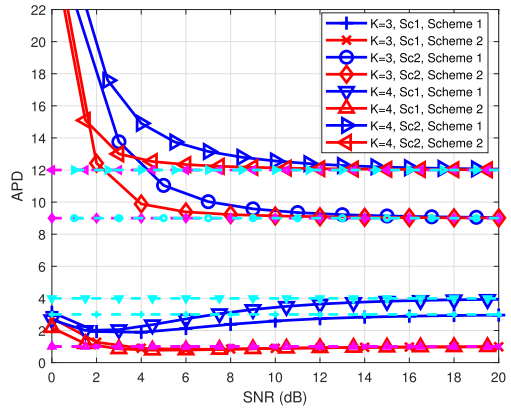

FIGURE 4. APD performance with $L = 4$. $(d_{SR}, d_{RD}) = (4, 2)$ km and $(d_{SR}, d_{RD}) = (2, 4)$ km in scenario 1 (Sc1) and scenario 2 (Sc2), respectively. Solid and dashes lines correspond to the exact and asymptotic values, respectively.

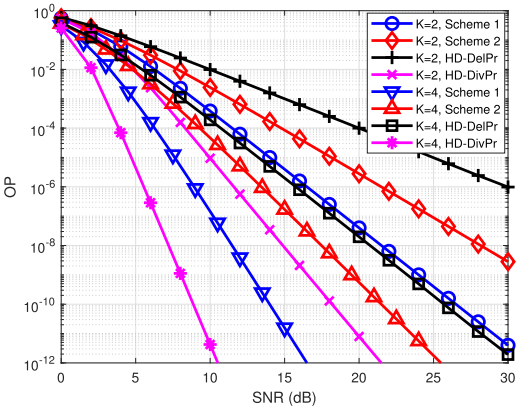

FIGURE 5. OP performance with $L = 5$, $d_{SR} = 4$ km and $d_{RD} = 2$ km.

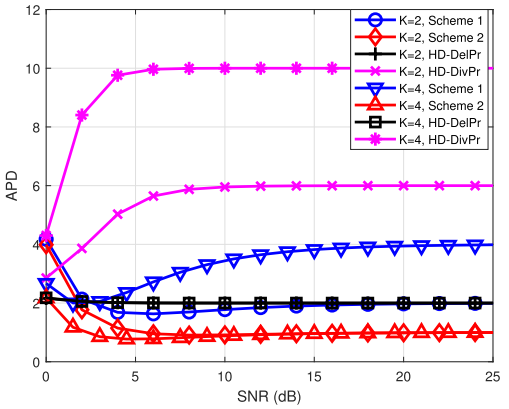

FIGURE 6. APD performance with $L = 5$, $d_{SR} = 4$ km and $d_{RD} = 2$ km.

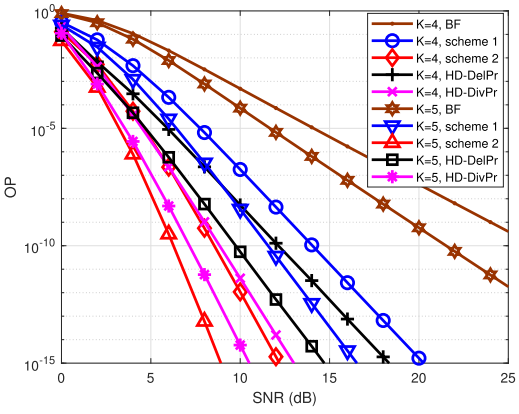

FIGURE 7. OP performance with $L = 2$, $d_{SR} = 3$ km and $d_{RD} = 4$ km.

APD values in Table 1. In scenario 1, scheme 2 achieves the smallest possible delay of 1 regardless of the number of relays while the APD of scheme 1 increases with K. In scenario 2, results in Fig. 4 validate the observation that both schemes yield the same asymptotic delay that increases with K.

Fig. 5 and Fig. 6 show the OP and APD performances, respectively, with $K = 2$ and $K = 4$ for $L = 5$ in the case where the relays are closer to D (q < p) with $d_{SR} = 4$ km and $d_{RD} = 2$ km. As a benchmark, we also show the performance of the threshold-based HD BA relaying protocol that was recently proposed in [5]. In particular, we consider two variants of this HD protocol. Namely, a delay-prioritizing scheme (HD-DelPr) that achieves the smallest possible asymptotic APD value of 2 at the expense of a deteriorated OP performance as well as a diversity-prioritizing scheme (HD-DivPr) that maximizes the diversity order with an increased asymptotic APD value of $2(K + 1)$. Results in Fig. 5 and Fig. 6 highlight on the advantages of the proposed FD relaying schemes that prioritize the communication along an available end-to-end link. In particular, scheme 2 outperforms HD-DelPr in both the outage and delay performances. While HD-DelPr severely penalizes the OP for the sake of minimizing the asymptotic delay to two, FD relays with scheme 2 can further reduce the asymptotic APD to the unprecedented value of one while concurrently reaping significant OP gains. Compared to HD-DelPr, scheme 1 achieves very high OP gains with a comparable delay performance with $K = 2$ and with double the delay with $K = 4$. For example, with $K = 2$ at $OP = 10^{-6}$, scheme 1 outperforms HD-DelPr by around 13.5 dB while achieving the same asymptotic APD value of 2. As for HD-DivPr, this scheme disregards the delay and suffers from excessive APD values that might not be acceptable for many applications. For example, while HD-DivPr outperforms scheme 1 by 5 dB and 3.5 dB at $OP = 10^{-6}$ with $K = 2$ and $K = 4$, respectively, the APD is increased 3 folds and 2.5 folds, respectively, to reach the very high value of 10 with $K = 4$.

Fig. 7 and Fig. 8 show the performance in the case where the relays are closer to S with $d_{SR} = 3$ km and $d_{RD} = 4$ km for $K \in \{4, 5\}$. Since the proposed relaying schemes attain the full advantage with buffer sizes not exceeding two, we fix $L = 2$. Results in Fig. 7 demonstrate the huge performance gains that can be achieved compared to buffer-free (BF) systems. In this context, for $K = 4$ at $OP = 10^{-5}$, equipping the relays with buffers allows to realize performance gains in the order of 6.5 dB and 9.5 dB by implementing scheme 1 and scheme 2, respectively. Comparing the proposed FD schemes shows that scheme 2 outperforms scheme 1 in terms of OP where the performance gap increases with K. From

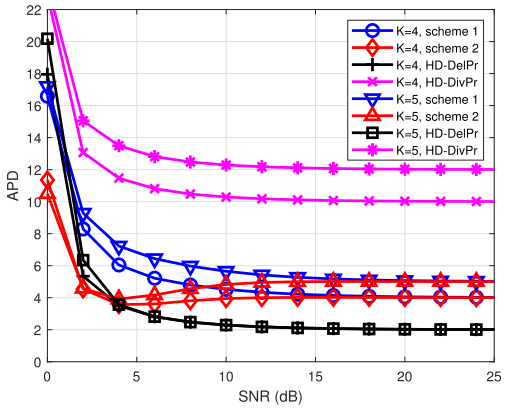

FIGURE 8. APD performance with $L = 2$, $d_{\mathrm{SR}} = 3$ km and $d_{\mathrm{RD}} = 4$ km.

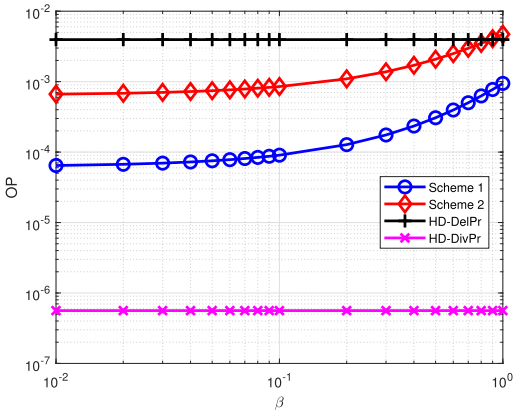

FIGURE 9. Impact of the residual SI on the OP with $K = 2$, $L = 5$, $d_{\mathrm{SR}} = 4$ km and $d_{\mathrm{RD}} = 2$ km.

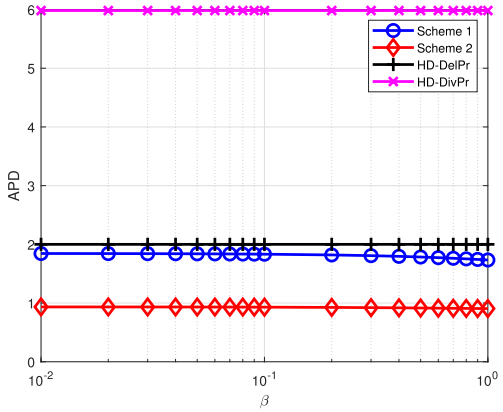

FIGURE 10. Impact of the residual SI on the APD with $K = 2$, $L = 5$, $d_{\mathrm{SR}} = 4$ km and $d_{\mathrm{RD}} = 2$ km.

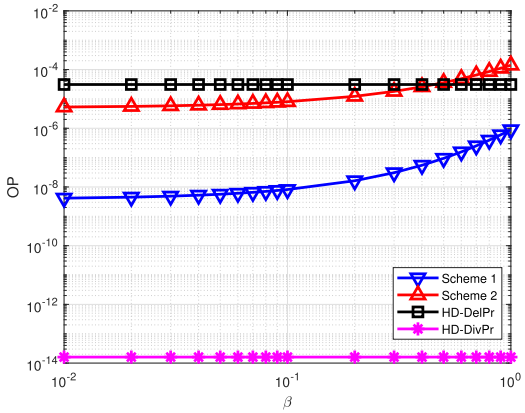

FIGURE 11. Impact of the residual SI on the OP with $K = 4$, $L = 5$, $d_{\mathrm{SR}} = 4$ km and $d_{\mathrm{RD}} = 2$ km.

Fig. 8, these OP gains are associated with slight improvement in the APD at low SNRs and with a comparable delay performance at average-to-large SNRs. Results show that scheme 2 reduces the OP not only compared to HD-DelPr the prioritizes the delay but also compared to HD-DivPr that is designed to minimize the OP. In this case, the gap between the asymptotic APD values of K and $2(K + 1)$ pertaining to scheme 2 and HD-DivPr increases with the number of relays. This highlights on the importance of deploying FD relays in cooperative networks for boosting the system's reliability with significantly reduced delays. Finally, it is worth highlighting that the performance improvements attained by the proposed schemes are associated with a reduced implementation complexity compared to HD-DelPr and HD-DivPr. In fact, while the signalling overhead of the proposed schemes involves only $2K$ bits for indicating the availabilities of the links, $K\lceil \log_2(L) \rceil$ additional bits must be fed back to the central node with HD-DelPr and HD-DivPr in order to indicate the states of the relays' buffers. As such, when K and L increase, the additional signalling overhead required by the HD BA schemes in [5] becomes more significant.

Fig. 9 and Fig. 10 highlight the impact of the residual SI on the performance with $K = 2$, $L = 5$, $d_{\mathrm{SR}} = 4$ km and $d_{\mathrm{RD}} = 2$ km. The OP and APD are plotted as a function of the SI parameter β at $\bar{\gamma} = 12$ dB. While the performances of the HD relaying schemes are independent of β, results in Fig. 9 highlight the OP degradations of the FD schemes when β increases while Fig. 10 demonstrates the marginal impact of SI on the APD that remains almost constant. While scheme 1 results in reduced OP levels compared to HD-DelPr for all values of β, the OP of scheme 2 exceeds that of HD-DelPr for the values of β above 0.9. For this range of values of β, the main advantage of scheme 2 resides in reducing the APD by a factor of 2 as can be observed from Fig. 10. The main conclusion that can be drawn from Fig. 9 and Fig. 10 is as follows: FD relaying ensures the streamlined flow of packets in the network resulting in reducing the queuing delays even with pronounced levels of residual SI. Moreover, the OP advantage is maintained for small-to-average values of β while large values of β significantly deteriorate the OP performance because of the increase in the outage probabilities of the S-R links. However, even with such deteriorations, the OP advantage with respect to HD relaying can be maintained (as for scheme 1) or marginally compromised only for very large values of β (as for scheme 2).

The simulation scenario in Fig. 9 and Fig. 10 is reproduced in Fig. 11 and Fig. 12 with $K = 4$ relays. For scheme 1, the findings in the absence of SI (Fig. 5 and Fig. 6) apply in

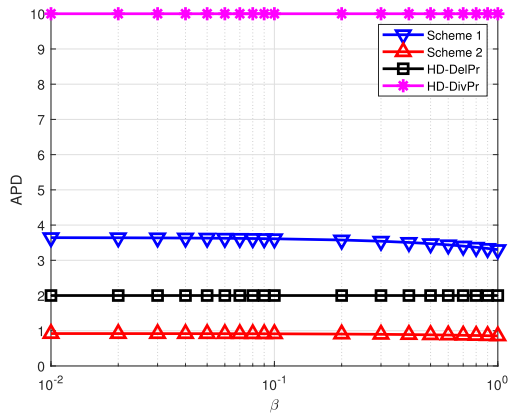

FIGURE 12. Impact of the residual SI on the APD with $K = 4$, $L = 5$, $d_{SR} = 4$ km and $d_{RD} = 2$ km.

the presence of SI as well. More specifically, for all values of β, scheme 1 reduces the OP compared to HD-DelPr at the expense of increased APDs. Compared to HD-DivPr, the APD advantage is obvious while the OP is compromised. From Fig. 12, scheme 2 maintains its predominant APD advantage compared to the HD schemes and the FD scheme 1 for all values of β. Compared to HD-DivPr, the APD is almost ten time smaller while, compared to HD-DelPr, the OP advantage is compromised for large values of β exceeding 0.5.

VI. CONCLUSION

Deploying FD relays allows to improve the performance of BA cooperative networks compared to the case where the relays abide to the HD constraint. In this work, we proposed two novel relaying schemes to reap these gains and we evaluated their asymptotic performance by identifying the subsets of states that dominate the asymptotic behaviour of the MC. The advantages of the proposed FD BA schemes compared to the state-of-the-art HD BA relaying strategies are delineated for different network setups. This opens the door for further investigating the problem of FD BA relaying with the objective of designing new relay selection strategies that can further reduce the OP, reduce the APD or achieve improved levels of tradeoff between OP and APD.

APPENDIX A

For $\mathfrak{q} \ll \mathfrak{p}$, an element $(l_1, \ldots, l_K)$ of the set $\mathcal{C} = \{0,1\}^K$ in (36) can be written as $\mathbf{s}_\Theta$ for any subset Θ of $\{1, \ldots, K\}$ where $l_k = 0$ for $k \in \Theta$ and $l_k = 1$ otherwise. From the definition of χ in (37), it follows that $|\Theta| = \chi$. From (4):

$$(l_k, q_k) = \begin{cases} (0,1), & k \in \Theta; \\ (1, \mathfrak{q}_k), & k \in \{1, \ldots, K\} \backslash \Theta. \end{cases} \tag{49}$$

Since $q_k = 1 \Rightarrow 1 - (1-p_k)(1-q_k) = 1$, then (5) can be written as:

$$t_{(l_1,\ldots,l_K),(l_1,\ldots,l_K)} \approx 1 - \prod_{k \in \{1,\ldots,K\} \backslash \Theta} [1 - (1 - \mathfrak{p}_k)(1 - \mathfrak{q}_k)] \tag{50}$$

$$\approx 1 - \prod_{k \in \{1,\ldots,K\} \backslash \Theta} [\mathfrak{p}_k] = 1 - \mathfrak{p}^{K-\chi}, \tag{51}$$

since $p_k = \mathfrak{p}_k = \mathfrak{p}$ for $k = 1, \ldots, K$ since $l_k \in \{0,1\}$ implying that none of the buffers is full. The approximation in (51) follows since $\mathfrak{q}_k \ll \mathfrak{p}_k$ following from $\mathfrak{q} \ll \mathfrak{p}$.

Since for elements of $\mathcal{C}$, $p_k = \mathfrak{p}_k$ and $1 - p_k = 1 - \mathfrak{p}_k \approx 1$, (6) can be written as:

$$t_{(l_1,\ldots,l_K),(l_1,\ldots,l_K)+\mathbf{e}_i} = q_i \sum_{\mathcal{A} \subset \{1,\ldots,K\} \backslash \{i\}} \sum_{\mathcal{S} \subset \bar{\mathcal{A}}} \frac{t_1 t_2 t_3}{|\mathcal{A}| + |\mathcal{S}| + 1}, \tag{52}$$

where $t_1 \triangleq \prod_{k \in \mathcal{A}} (1 - q_k) \mathfrak{p}_k$, $t_2 \triangleq \prod_{k' \in \bar{\mathcal{A}}} q_{k'}$ and $t_3 \triangleq \prod_{j' \in \bar{\mathcal{A}} \backslash \mathcal{S}} \mathfrak{p}_{j'}$.

For $i \notin \Theta$, $q_i = \mathfrak{q}_i = \mathfrak{q}$ implying that (52) tends to zero since $\mathfrak{q} \ll 1$. Consider now the case $i \in \Theta$. In this case, the term q_i in (52) is equal to 1. For the term t_1 to be different from zero, $\mathcal{A} \cap \Theta = \phi$ since for an element k of Θ, $q_k = 1$ implying that $1 - q_k = 0 \Rightarrow t_1 = 0$. For t_2 to be equal to 1 (and not a higher power of $\mathfrak{q}$ that is negligible), $\bar{\mathcal{A}} = \{1, \ldots, K\} \backslash \{i\} \backslash \mathcal{A} \subset \Theta$. The conditions $\mathcal{A} \cap \Theta = \phi$ and $\bar{\mathcal{A}} \subset \Theta$ can be concurrently satisfied if:

$$\mathcal{A} = \{1, \ldots, K\} \backslash \Theta \Rightarrow \bar{\mathcal{A}} = \Theta \backslash \{i\}, \tag{53}$$

resulting in $t_1 = \mathfrak{p}^{K-\chi}$, $t_2 = 1$ and $|\mathcal{A}| = K - \chi$. On the other hand, in order to minimize t_3 and identify the most probable asymptotic transition:

$$\bar{\mathcal{A}} \backslash \mathcal{S} = \phi \Rightarrow \mathcal{S} = \bar{\mathcal{A}} = \Theta \backslash \{i\}, \tag{54}$$

resulting in $t_3 = 1$ and $|\mathcal{S}| = \chi - 1$. Replacing t_1, t_2, t_3, $|\mathcal{A}|$ and $|\mathcal{S}|$ by their values in (52) results in:

$$t_{(l_1,\ldots,l_K),(l_1,\ldots,l_K)+\mathbf{e}_i} = \begin{cases} 0, & i \notin \Theta; \\ \dfrac{1}{K} \mathfrak{p}^{K-\chi}, & i \in \Theta. \end{cases} \tag{55}$$

Similarly, (7) can be written as:

$$t_{(l_1,\ldots,l_K),(l_1,\ldots,l_K)-\mathbf{e}_i} = (1 - q_i) \mathfrak{p}_i \times \sum_{\mathcal{A} \subset \{1,\ldots,K\} \backslash \{i\}} \sum_{\mathcal{S} \subset \bar{\mathcal{A}}} \frac{r_1 r_2 r_3 r_4}{|\mathcal{A}| + |\mathcal{S}| + 1}, \tag{56}$$

where $r_1 \triangleq \prod_{k \in \mathcal{A}} (1 - \mathfrak{p}_k) q_k \approx \prod_{k \in \mathcal{A}} q_k$, $r_2 \triangleq \prod_{k' \in \bar{\mathcal{A}}} \mathfrak{p}_{k'}$, $r_3 \triangleq \prod_{j \in \mathcal{S}} (1 - q_j)$ and $r_4 \triangleq \prod_{j' \in \bar{\mathcal{A}} \backslash \mathcal{S}} q_{j'}$.

For $i \in \Theta$, $q_i = 1$ implying that the transition probability in (56) is equal to zero. Consider the case $i \notin \Theta$. In this case, $1 - q_i = 1 - \mathfrak{q} \approx 1$. For r_1 to be equal to one (i.e. a nonzero power of $\mathfrak{q}$), $\mathcal{A} \subset \Theta$. For r_3 and r_4 to be different from zero, $\mathcal{S} \subset \{1, \ldots, K\} \backslash \Theta$ and $\bar{\mathcal{A}} \backslash \mathcal{S} \subset \Theta$, respectively. The conditions $\mathcal{A} \subset \Theta$, $\mathcal{S} \subset \{1, \ldots, K\} \backslash \Theta$ and $\bar{\mathcal{A}} \backslash \mathcal{S} \subset \Theta$ can be concurrently met if and only if:

$$\bar{\mathcal{A}} \backslash \mathcal{S} = \mathcal{A} = \Theta \Rightarrow \mathcal{S} = \bar{\mathcal{A}} = \{1, \ldots, K\} \backslash \{i\} \backslash \Theta, \tag{57}$$

resulting in $|\mathcal{A}| = \chi$, $|\mathcal{S}| = K-1-\chi$, $r_1 = r_3 = r_4 = 1$ and $r_2 = \mathfrak{p}^{K-1-\chi}$. Replacing in (56) results in:

$$t_{(l_1,\ldots,l_K),(l_1,\ldots,l_K)-\mathbf{e}_i} = \begin{cases} 0, & i \in \Theta; \\ \frac{1}{K}\mathfrak{p}^{K-\chi}, & i \notin \Theta. \end{cases} \tag{58}$$

Among the transitions in (51), (55) and (58), only the transition $(l_1,\ldots,l_K) \rightarrow (l_1,\ldots,l_K)+\mathbf{e}_i$ for $i \notin \Theta$ might lead from an element inside $\mathcal{C}$ to an element outside $\mathcal{C}$. Since this transition occurs with a probability that tends to zero asymptotically following from (55), then we can deduce that the set $\mathcal{C}$ is closed when $\mathfrak{q}$ can be neglected compared to $\mathfrak{p}$.

By considering the elements of $\mathcal{C}$, the balance equation at a state $\mathbf{s}_\Theta$ of $\mathcal{C}$ can be written as follows following from (10):

$$\pi_{\mathbf{s}_\Theta} = t_{\mathbf{s}_\Theta,\mathbf{s}_\Theta}\pi_{\mathbf{s}_\Theta} + \sum_{i\in\Theta} t_{\mathbf{s}_\Theta+\mathbf{e}_i,\mathbf{s}_\Theta}\pi_{\mathbf{s}_\Theta+\mathbf{e}_i} + \sum_{j\in\{1,\ldots,K\}\setminus\Theta} t_{\mathbf{s}_\Theta-\mathbf{e}_j,\mathbf{s}_\Theta}\pi_{\mathbf{s}_\Theta-\mathbf{e}_j}. \tag{59}$$

From (51), $t_{\mathbf{s}_\Theta,\mathbf{s}_\Theta} = 1-\mathfrak{p}^{K-\chi}$. From (58), $t_{\mathbf{s}_\Theta+\mathbf{e}_i,\mathbf{s}_\Theta} = \frac{1}{K}\mathfrak{p}^{K-(\chi-1)}$ since when $\mathbf{s}_\Theta$ contains χ zero components, the state $\mathbf{s}_\Theta+\mathbf{e}_i$ for $i \in \Theta$ will contain one less zero component. Moreover, $\mathbf{s}_\Theta + \mathbf{e}_i = \mathbf{s}_{\Theta\setminus\{i\}}$ implying that $i \notin \Theta\setminus\{i\}$ and, hence, the second condition in (58) holds. Similarly, from (55), $t_{\mathbf{s}_\Theta-\mathbf{e}_j,\mathbf{s}_\Theta} = \frac{1}{K}\mathfrak{p}^{K-(\chi+1)}$ since $\mathbf{s}_\Theta - \mathbf{e}_j$ for $j \notin \Theta$ contains $\chi+1$ zero elements. Moreover, $\mathbf{s}_\Theta - \mathbf{e}_j = \mathbf{s}_{\Theta\cup\{j\}}$ implying that $j \in \Theta\cup\{j\}$ and, hence, the second condition in (55) holds. Therefore, (59) can be written as:

$$\mathfrak{p}^{K-\chi}\pi_{\mathbf{s}_\Theta} = \frac{1}{K}\sum_{i\in\Theta}\mathfrak{p}^{K-\chi+1}\pi_{\mathbf{s}_\Theta\setminus\{i\}} + \frac{1}{K}\sum_{j\in\{1,\ldots,K\}\setminus\Theta}\mathfrak{p}^{K-\chi-1}\pi_{\mathbf{s}_\Theta\cup\{j\}}, \tag{60}$$

where $\chi = |\Theta|$. For the relation in (60) to hold for all subsets Θ of $\{1,\ldots,K\}$, the steady-state probability of a state written as $\mathbf{s}_\mathcal{S}$ must be equal to $\mathfrak{p}^{|\mathcal{S}|}$. In fact, replacing $\pi_{\mathbf{s}_\Theta} = \mathfrak{p}^{|\Theta|} = \mathfrak{p}^\chi$, $\pi_{\mathbf{s}_\Theta\setminus\{i\}} = \mathfrak{p}^{\chi-1}$ and $\pi_{\mathbf{s}_\Theta\cup\{j\}} = \mathfrak{p}^{\chi+1}$ in (60) results in the relation $\mathfrak{p}^K = \frac{1}{K}\sum_{i\in\Theta}\mathfrak{p}^K + \frac{1}{K}\sum_{j\in\{1,\ldots,K\}\setminus\Theta}\mathfrak{p}^K$ that is always satisfied for any $\Theta \subset \{1,\ldots,K\}$.

In order to further refine the approximate asymptotic results and end up with steady-state probabilities that add up to one, we propose to multiply the steady-state probability $\mathfrak{p}^\chi$ of the state $\mathbf{s}_\Theta$ by the term $(1-\mathfrak{p})^{K-\chi}$ which results in the first expression provided in (37). This refinement holds since $(1-\mathfrak{p})^{K-\chi} = 1$ for $\chi = K$ and $(1-\mathfrak{p})^{K-\chi} \approx 1-(K-\chi)\mathfrak{p} \approx 1$ when $\chi \neq K$ since $\mathfrak{p} \ll 1$ for asymptotically large values of the SNR.

Consider now the case $\mathfrak{p} \ll \mathfrak{q}$. An element $(l_1,\ldots,l_K)$ of $\mathcal{C} = \{L-1, L\}^K$ in (36) can be written as $\mathbf{s}_\Theta$ for $\Theta \subset \{1,\ldots,K\}$ where $l_k = L$ for $k \in \Theta$ and $l_k = L-1$ otherwise. Therefore, from (3), $p_k = 1$ for $k \in \Theta$ and $p_k = \mathfrak{p}_k = \mathfrak{p}$ for $k \notin \Theta$. Similar to (51):

$$t_{(l_1,\ldots,l_K),(l_1,\ldots,l_K)} = 1-\mathfrak{q}^{K-\psi}, \tag{61}$$

where $\psi = |\Theta|$. Equation (61) follows since $1-(1-p_k)(1-q_k) \approx \mathfrak{p}_k+\mathfrak{q}_k \approx \mathfrak{q}_k = \mathfrak{q}$ for $k \notin \Theta$ and $1-(1-p_k)(1-q_k) = 1$ for $k \in \Theta$. Note that $q_1 = \cdots = q_K = \mathfrak{q}$ for elements of $\mathcal{C}$ since none of the buffers is empty.

Since (7) can be obtained from (6) by interchanging the roles of the unavailability probabilities p_k and q_k, then the analysis of the transition $(l_1,\ldots,l_K) \rightarrow (l_1,\ldots,l_K)+\mathbf{e}_i$ with $\mathfrak{p} \ll \mathfrak{q}$ is equivalent to the presented analysis for the transition $(l_1,\ldots,l_K) \rightarrow (l_1,\ldots,l_K)-\mathbf{e}_i$ in the case $\mathfrak{q} \ll \mathfrak{p}$. Therefore, replacing $\mathfrak{p}$ by $\mathfrak{q}$ in (58) results in:

$$t_{(l_1,\ldots,l_K),(l_1,\ldots,l_K)+\mathbf{e}_i} = \begin{cases} 0, & i \in \Theta; \\ \frac{1}{K}\mathfrak{q}^{K-\psi}, & i \notin \Theta. \end{cases} \tag{62}$$

Similarly, $t_{(l_1,\ldots,l_K),(l_1,\ldots,l_K)-\mathbf{e}_i}$ for $\mathfrak{p} \ll \mathfrak{q}$ is equivalent to $t_{(l_1,\ldots,l_K),(l_1,\ldots,l_K)+\mathbf{e}_i}$ for $\mathfrak{q} \ll \mathfrak{p}$ which from (55) implies that:

$$t_{(l_1,\ldots,l_K),(l_1,\ldots,l_K)-\mathbf{e}_i} = \begin{cases} 0, & i \notin \Theta; \\ \frac{1}{K}\mathfrak{q}^{K-\psi}, & i \in \Theta. \end{cases} \tag{63}$$

where the first condition in (63) implies that the set $\mathcal{C} = \{L-1, L\}^K$ is closed. Similar to (59)-(60), the balance equations at elements of $\mathcal{C}$ can be written as:

$$\pi_{\mathbf{s}_\Theta} = \underbrace{t_{\mathbf{s}_\Theta,\mathbf{s}_\Theta}}_{=1-\mathfrak{q}^{K-\psi}}\pi_{\mathbf{s}_\Theta} + \sum_{i\in\{1,\ldots,K\}\setminus\Theta}\underbrace{t_{\mathbf{s}_\Theta+\mathbf{e}_i,\mathbf{s}_\Theta}}_{=\frac{1}{K}\mathfrak{q}^{K-(\psi+1)}}\pi_{\mathbf{s}_\Theta\cup\{i\}} + \sum_{j\in\Theta}\underbrace{t_{\mathbf{s}_\Theta-\mathbf{e}_j,\mathbf{s}_\Theta}}_{=\frac{1}{K}\mathfrak{q}^{K-(\psi-1)}}\pi_{\mathbf{s}_\Theta\setminus\{j\}}, \tag{64}$$

which holds for any set $\Theta \subset \{1,\ldots,K\}$ if $\pi_{\mathbf{s}_\mathcal{S}} = \mathfrak{q}^{|\mathcal{S}|} \approx \mathfrak{q}^{|\mathcal{S}|}(1-\mathfrak{q})^{K-|\mathcal{S}|}$ resulting in the second expression in (37).

APPENDIX B

Consider the case $\mathfrak{q} \ll \mathfrak{p}$. As in Appendix A, denote by $\mathbf{s}_\Theta$ the state $(l_1,\ldots,l_K)$ such that $l_k = 0$ (resp. $l_k = 1$) for $k \in \Theta$ (resp. $k \notin \Theta$) for any $\Theta \subset \{1,\ldots,K\}$ where $|\Theta| \triangleq \chi$ and (49) holds. Similar to (51), the probability of self transition tends to the following asymptotic value:

$$t_{(l_1,\ldots,l_K),(l_1,\ldots,l_K)} = 1-\mathfrak{p}^{K-\chi}. \tag{65}$$

Consider the transition $(l_1,\ldots,l_K) \rightarrow (l_1,\ldots,l_K)+\mathbf{e}_i$. When $(l_1,\ldots,l_K)$ is different from the all-zero state, at least one buffer is not empty implying that at least one unavailability probability in $\{q_k\}_{k=1}^K$ is equal to $\mathfrak{q}$. As such, the multiplicative term $\prod_{k=1}^K q_k$ in (8) will be equal to a nonzero power of $\mathfrak{q}$ implying that $t_{(l_1,\ldots,l_K),(l_1,\ldots,l_K)+\mathbf{e}_i} \rightarrow 0$ in this case since $\mathfrak{q} \ll 1$. For $(l_1,\ldots,l_K) = (0,\ldots,0)$, $q_1 = \cdots = q_K = 1$ implying that (8) can be written as (for $i = 1,\ldots,K$):

$$t_{(0,\ldots,0),\mathbf{e}_i} = \sum_{\mathcal{S}\subset\{1,\ldots,K\}\setminus\{i\}}\frac{1}{|\mathcal{S}|+1}\prod_{j'\in\bar{\mathcal{S}}=\{1,\ldots,K\}\setminus\{i\}\setminus\mathcal{S}}\mathfrak{p}_{j'}, \tag{66}$$

where terms of the form $1-p_k$ were replaced by 1 in (8) since $1-p_k = 1-\mathfrak{p}_k \approx 1$.

The term with the largest probability in (66) corresponds to $\bar{\mathcal{S}} = \phi$ that implies that $\mathcal{S} = \{1, \ldots, K\}\backslash\{i\}$ and $|\mathcal{S}| = K-1$. Replacing in (66) results in $t_{(0,\ldots,0),\mathbf{e}_i} \rightarrow \frac{1}{K}$. Therefore:

$$t_{(l_1,\ldots,l_K),(l_1,\ldots,l_K)+\mathbf{e}_i} = \begin{cases} 0, & (l_1,\ldots,l_K) \neq (0,\ldots,0); \\ \dfrac{1}{K}, & (l_1,\ldots,l_K) = (0,\ldots,0). \end{cases} \tag{67}$$

Consider now the transition $(l_1, \ldots, l_K) \rightarrow (l_1, \ldots, l_K) - \mathbf{e}_i$. Equation (9) can be written as:

$$t_{(l_1,\ldots,l_K),(l_1,\ldots,l_K)-\mathbf{e}_i} = (1-q_i)\mathfrak{p}_i \sum_{\mathcal{A}\subset\{1,\ldots,K\}\backslash\{i\}} \frac{t_1 t_2}{|\mathcal{A}|+1}, \tag{68}$$

where $t_1 \triangleq \prod_{k\in\mathcal{A}}[(1-q_k)\mathfrak{p}_k$ and $t_2 \triangleq \prod_{k'\in\bar{\mathcal{A}}} q_{k'}$ and where the S-R unavailability probabilities were replaced by the corresponding outage probabilities.

For $i \in \Theta$, $q_i = 1$ implying that $t_{(l_1,\ldots,l_K),(l_1,\ldots,l_K)-\mathbf{e}_i} = 0$. Consider next the case $i \notin \Theta$. For the term t_1 to be different from zero, $\mathcal{A}\cap\Theta = \phi$. For the term t_2 to be equal to 1 (and not a nonzero power of $\mathfrak{q}$ that is negligible), $\bar{\mathcal{A}} \subset \Theta$. The above conditions can be concurrently satisfied if $\bar{\mathcal{A}} = \Theta$ implying that $\mathcal{A} = \{1, \ldots, K\}\backslash\{i\}\backslash\Theta$ which results in $t_1 = \mathfrak{p}^{K-1-\chi}$, $t_2 = 1$ and $|\mathcal{A}| = K-1-\chi$. Replacing in (68) results in:

$$t_{(l_1,\ldots,l_K),(l_1,\ldots,l_K)-\mathbf{e}_i} = \begin{cases} 0, & i \in \Theta; \\ \dfrac{1}{K-\chi}\mathfrak{p}^{K-\chi}, & i \notin \Theta. \end{cases} \tag{69}$$

Equations (67) and (69) imply that transitions from states inside $\{0, 1\}^K$ to other states outside this set can be neglected (since they occur with probabilities that include nonzero powers of $\mathfrak{q} \ll 1$) implying that this set is closed. Moreover, among the elements of $\{0, 1\}^K$, the transition probability in (69) is the highest when $\chi = K-1$ for which $t_{(l_1,\ldots,l_K),(l_1,\ldots,l_K)-\mathbf{e}_i} = \mathfrak{p}$ for $i \notin \Theta$. The relation $\chi = K-1$ implies that $K-1$ components of $(l_1, \ldots, l_K)$ are equal to zero and, hence, the dominant states are given by $\{\mathbf{e}_k\}_{k=1}^K$. Adding the all-zero state to this set (following from (67)) results in the expression of the closed-subset $\mathcal{C}$ provided in (40). Note that the highest probability in (69) is attained for $\chi = K-1$ and not $\chi = K$. In fact, $\chi = K$ implies that $(l_1, \ldots, l_K) = (0, \ldots, 0)$ and $\Theta = \{1, \ldots, K\}$ implying that $t_{(l_1,\ldots,l_K),(l_1,\ldots,l_K)-\mathbf{e}_i} = 0$ and the corresponding transition is not possible since $i \in \Theta$ for any i.

Therefore, following from (65), (67) and (69), the nonzero transition probabilities among elements of $\mathcal{C}$ are given by (for $k = 1, \ldots, K$):

$$\begin{cases} t_{\mathbf{z},\mathbf{z}} = 0 \\ t_{\mathbf{z},\mathbf{e}_k} = \dfrac{1}{K} \end{cases} ; \quad \begin{cases} t_{\mathbf{e}_k,\mathbf{e}_k} = 1-\mathfrak{p} \\ t_{\mathbf{e}_k,\mathbf{z}} = \mathfrak{p} \end{cases}, \tag{70}$$

where $\mathbf{z} \triangleq (0, \ldots, 0)$.

Since the transition probabilities in (70) do not depend on k, then $\pi_{\mathbf{e}_1} = \cdots = \pi_{\mathbf{e}_K} = \frac{1-\pi_{\mathbf{z}}}{K}$ where the last equality follows since the total steady-state probability should be equal to 1. Replacing (70) in (10), the balance equation at the state $\mathbf{z}$ is given by $\pi_{\mathbf{z}} = \mathfrak{p}\pi_{\mathbf{e}_1} + \cdots + \mathfrak{p}\pi_{\mathbf{e}_K}$. Solving the above relations results in the asymptotic steady-state distribution provided in (41).

APPENDIX C

Consider the case $\mathfrak{p} \ll \mathfrak{q}$. As in Appendix A, denote by $\mathbf{s}_\Theta$ the state $(l_1, \ldots, l_K)$ such that $l_k = L$ (resp. $l_k = L-1$) for $k \in \Theta$ (resp. $k \notin \Theta$) for any $\Theta \subset \{1, \ldots, K\}$ and let $\psi = |\Theta|$. Similar to (61), the probability of self transition is given by:

$$t_{(l_1,\ldots,l_K),(l_1,\ldots,l_K)} = 1 - \mathfrak{q}^{K-\psi}. \tag{71}$$

Consider the transition $(l_1, \ldots, l_K) \rightarrow (l_1, \ldots, l_K) + \mathbf{e}_i$. For $i \in \Theta$, $p_i = 1$ implying that $t_{(l_1,\ldots,l_K),(l_1,\ldots,l_K)+\mathbf{e}_i} = 0$ following from (8). For $i \notin \Theta$, (8) can be written as:

$$t_{(l_1,\ldots,l_K),(l_1,\ldots,l_K)+\mathbf{e}_i} = \left[\prod_{k=1}^{K} \mathfrak{q}_k\right] \sum_{\mathcal{S}\subset\{1,\ldots,K\}\backslash\{i\}} \frac{t_1 t_2}{|\mathcal{S}|+1}, \tag{72}$$

where $t_1 \triangleq \prod_{j\in\mathcal{S}}(1-p_j)$ and $t_2 \triangleq \prod_{j'\in\bar{\mathcal{S}}} p_{j'}$. In (72), q_k was replaced by $\mathfrak{q}_k$ for $k = 1, \ldots, K$ since none of the buffers is empty. For t_1 to be different from zero, $\mathcal{S}\cap\Theta = \phi$. For t_2 to be equal to 1 (and not $\mathfrak{p}^n$ with $n \neq 0$), $\bar{\mathcal{S}} \subset \Theta$. The above conditions can concurrently hold if $\bar{\mathcal{S}} = \Theta$ implying that $\mathcal{S} = \{1, \ldots, K\}\backslash\{i\}\backslash\Theta \Rightarrow |\mathcal{S}| = K-1-\psi$. Replacing in (72) results in:

$$t_{(l_1,\ldots,l_K),(l_1,\ldots,l_K)+\mathbf{e}_i} = \begin{cases} 0 & i \in \Theta; \\ \dfrac{1}{K-\psi}\mathfrak{q}^K, & i \notin \Theta. \end{cases} \tag{73}$$

Consider the transition $(l_1, \ldots, l_K) \rightarrow (l_1, \ldots, l_K) - \mathbf{e}_i$. For $i \notin \Theta$, $p_i = \mathfrak{p}$ implying that $t_{(l_1,\ldots,l_K),(l_1,\ldots,l_K)-\mathbf{e}_i} \rightarrow 0$ following from (9) since $\mathfrak{p} \ll 1$. For $i \in \Theta$, (9) can be written as:

$$t_{(l_1,\ldots,l_K),(l_1,\ldots,l_K)-\mathbf{e}_i} = (1-\mathfrak{q}_i) \sum_{\mathcal{A}\subset\{1,\ldots,K\}\backslash\{i\}} \frac{r_1 r_2}{|\mathcal{A}|+1}, \tag{74}$$

where $r_1 \triangleq \prod_{k\in\mathcal{A}}(1-\mathfrak{q}_k)p_k$ and $r_2 \triangleq \prod_{k'\in\bar{\mathcal{A}}} \mathfrak{q}_{k'}$. For r_1 to be different from zero, $\mathcal{A} \subset \Theta\backslash\{i\}$. In this case, r_2 assumes the largest possible value (i.e. the smallest power of $\mathfrak{q}$) when $\mathcal{A} = \Theta\backslash\{i\}$ implying that $\bar{\mathcal{A}} = \{1, \ldots, K\}\backslash\{i\}\backslash\Theta = \{1, \ldots, K\}\backslash\Theta$ since $i \in \Theta$. Therefore, $|\mathcal{A}| = \psi - 1$, $r_1 = (1-\mathfrak{q})^{\psi-1}$ and $r_2 = \mathfrak{q}^{K-\psi}$. Replacing these values in (74) results in:

$$t_{(l_1,\ldots,l_K),(l_1,\ldots,l_K)-\mathbf{e}_i} = \begin{cases} 0, & i \notin \Theta; \\ \dfrac{1}{\psi}\mathfrak{q}^{K-\psi}(1-\mathfrak{q})^{\psi} \approx \dfrac{1}{\psi}\mathfrak{q}^{K-\psi}, & i \in \Theta. \end{cases} \tag{75}$$

The fact that $t_{(l_1,\ldots,l_K),(l_1,\ldots,l_K)-\mathbf{e}_i} = 0$ for $i \notin \Theta$ implies that the set $\mathcal{C}$ in (44) is closed asymptotically since the transitions $(l_1, \ldots, l_K) \rightarrow (l_1, \ldots, l_K) + \mathbf{e}_i$ for $i \notin \Theta$ in (73) and $(l_1, \ldots, l_K) \rightarrow (l_1, \ldots, l_K) - \mathbf{e}_i$ for $i \in \Theta$ in (75) are confined within $\mathcal{C}$.

Since the transition probabilities in (71), (73) and (75) depend on ψ and not on the particular value of the set Θ,

then the states $\mathbf{s}_\Theta = L\sum_{k\in\Theta}\mathbf{e}_k + (L-1)\sum_{k'\in\{1,\ldots,K\}\setminus\Theta}\mathbf{e}_{k'}$ with the same value of $|\Theta|$ can be lumped together in the new state $\mathbf{g}_\psi$ such that $\psi = |\Theta|$. In this case, $\mathbf{g}_\psi$ corresponds to a group of $\binom{K}{\psi}$ states $\mathbf{s}_\Theta$ as follows:

$$\mathbf{g}_\psi = \{\mathbf{s}_\Theta \ ; \ |\Theta| = \psi\}. \tag{76}$$

From (71), (73) and (75), the transition probabilities among the lumped states $\{\mathbf{g}_\psi\}_{\psi=0}^{K}$ can be determined from:

$$t_{\mathbf{g}_\psi,\mathbf{g}_\psi} = 1 - \mathfrak{q}^{K-\psi}, \tag{77}$$

$$t_{\mathbf{g}_\psi,\mathbf{g}_{\psi+1}} = \sum_{i\in\{1,\ldots,K\}\setminus\Theta} \frac{1}{K-\psi}\mathfrak{q}^K = \mathfrak{q}^K \ ; \ \psi \neq K, \tag{78}$$

$$t_{\mathbf{g}_\psi,\mathbf{g}_{\psi-1}} = \sum_{i\in\Theta} \frac{1}{\psi}\mathfrak{q}^{K-\psi} = \mathfrak{q}^{K-\psi} \ ; \ \psi \neq 0. \tag{79}$$

Consequently, the balance equations at $\{\mathbf{g}_\psi\}_{\psi=0}^{K}$ are given by the following relations where π'_ψ stands for the steady-state probability of the lumped state $\mathbf{g}_\psi$:

$$\mathfrak{q}^K\pi'_0 = \mathfrak{q}^{K-1}\pi'_1, \tag{80}$$

$$\mathfrak{q}^{K-\psi}\pi'_\psi = \mathfrak{q}^K\pi'_{\psi-1} + \mathfrak{q}^{K-\psi-1}\pi'_{\psi+1} \ ; \ \psi = 1,\ldots,K-1, \tag{81}$$

$$\pi'_K = \mathfrak{q}^K\pi'_{K-1}. \tag{82}$$

In order to satisfy (80)-(82), we propose an asymptotic solution of the form:

$$\begin{cases} \pi'_0 = 1 \\ \pi'_k = \mathfrak{q}^k\pi'_{k-1} \quad \text{for } k = 1,\ldots,K \end{cases}. \tag{83}$$

For $k = 1$, (83) yields $\pi'_1 = \mathfrak{q}\pi'_0$ that is consistent with (80). For $k = K$, (83) yields $\pi'_K = \mathfrak{q}^K\pi'_{K-1}$ that is consistent with (82). Invoking (83) in (81) implies that:

$$\mathfrak{q}^{K-\psi}[\mathfrak{q}^\psi\pi'_{\psi-1}] = \mathfrak{q}^K\pi'_{\psi-1} + \mathfrak{q}^{K-\psi-1}[\mathfrak{q}^{\psi+1}\mathfrak{q}^\psi\pi'_{\psi-1}]; \quad \psi = 1,\ldots,K-1, \tag{84}$$

which implies that $\mathfrak{q}^K = \mathfrak{q}^K + \mathfrak{q}^{K+\psi}$ where this relation is true for asymptotically large values of the SNR since $\mathfrak{q}^{K+\psi}$ can be ignored compared to $\mathfrak{q}^K$ since $\psi \geq 1$ in (84) and $\mathfrak{q} \ll 1$.

The solution of (83) is $\pi'_\psi = \mathfrak{q}^\psi\mathfrak{q}^{\psi-1}\cdots\mathfrak{q}\pi'_0 = \mathfrak{q}^{\frac{\psi(\psi+1)}{2}}$ for $\psi = 1,\ldots,K$ and $\pi'_0 = 1 \approx 1 - \sum_{k=1}^{K}\mathfrak{q}^{\frac{k(k+1)}{2}}$ for $\mathfrak{q} \ll 1$ where the last approximation was applied so that $\sum_{k=0}^{K}\pi'_k = 1$. Dividing the probability π'_ψ among the $\binom{K}{\psi}$ states lumped in $\mathbf{g}_\psi$ results in the steady-state distribution provided in (45).

REFERENCES

[1] M. Agiwal, A. Roy, and N. Saxena, "Next generation 5G wireless networks: A comprehensive survey," *IEEE Commun. Surveys Tuts.*, vol. 18, no. 3, pp. 1617–1655, 3rd Quart., 2016.

[2] N. Nomikos, T. Charalambous, I. Krikidis, D. N. Skoutas, D. Vouyioukas, M. Johansson, and C. Skianis, "A survey on buffer-aided relay selection," *IEEE Commun. Surveys Tuts.*, vol. 18, no. 2, pp. 1073–1097, 2nd Quart., 2016.

[3] I. Krikidis, T. Charalambous, and J. S. Thompson, "Buffer-aided relay selection for cooperative diversity systems without delay constraints," *IEEE Trans. Wireless Commun.*, vol. 11, no. 5, pp. 1957–1967, May 2012.

[4] S. Luo and K. C. Teh, "Buffer state based relay selection for buffer-aided cooperative relaying systems," *IEEE Trans. Wireless Commun.*, vol. 14, no. 10, pp. 5430–5439, Oct. 2015.

[5] S. El-Zahr and C. Abou-Rjeily, "Threshold based relay selection for buffer-aided cooperative relaying systems," *IEEE Trans. Wireless Commun.*, vol. 20, no. 9, pp. 6210–6223, Sep. 2021.

[6] M. M. Razlighi and N. Zlatanov, "Buffer-aided relaying for the two-hop full-duplex relay channel with self-interference," *IEEE Trans. Wireless Commun.*, vol. 17, no. 1, pp. 477–491, Jan. 2018.

[7] S. M. Kim and M. Bengtsson, "Virtual full-duplex buffer-aided relaying in the presence of inter-relay interference," *IEEE Trans. Wireless Commun.*, vol. 15, no. 4, pp. 2966–2980, Apr. 2016.

[8] Y. Shin and S. J. Baek, "Cooperative buffer-aided relaying using full-duplex relays with flow control," *IEEE Trans. Veh. Technol.*, vol. 68, no. 2, pp. 1824–1838, Feb. 2019.

[9] D. Qiao, "Effective capacity of buffer-aided full-duplex relay systems with selection relaying," *IEEE Trans. Commun.*, vol. 64, no. 1, pp. 117–129, Jan. 2016.

[10] K. T. Phan and T. Le-Ngoc, "Power allocation for buffer-aided full-duplex relaying with imperfect self-interference cancelation and statistical delay constraint," *IEEE Access*, vol. 4, pp. 3961–3974, 2016.

[11] O. M. Kandelusy and N. J. Kirsch, "Full-duplex buffer-aided MIMO relaying networks: Joint antenna selection and rate allocation based on buffer status," *IEEE Netw. Lett.*, vol. 4, no. 3, pp. 99–103, Sep. 2022.

[12] N. Nomikos, T. Charalambous, D. Vouyioukas, R. Wichman, and G. K. Karagiannidis, "Integrating broadcasting and NOMA in full-duplex buffer-aided opportunistic relay networks," *IEEE Trans. Veh. Technol.*, vol. 69, no. 8, pp. 9157–9162, Aug. 2020.

[13] C. Li, P. Hu, Y. Yao, B. Xia, and Z. Chen, "Optimal multi-user scheduling for the unbalanced full-duplex buffer-aided relay systems," *IEEE Trans. Wireless Commun.*, vol. 18, no. 6, pp. 3208–3221, Jun. 2019.

[14] G. Liu, F. R. Yu, H. Ji, V. C. M. Leung, and X. Li, "In-band full-duplex relaying: A survey, research issues and challenges," *IEEE Commun. Surveys Tuts.*, vol. 17, no. 2, pp. 500–524, 2nd Quart., 2015.

[15] D. Dixit and P. R. Sahu, "Exact closed-form ABER for multi-hop regenerative relay systems over κ-μ fading," *IEEE Wireless Commun. Lett.*, vol. 6, no. 2, pp. 246–249, Apr. 2017.

[16] C. Abou-Rjeily and W. Fawaz, "Buffer-aided relaying protocols for cooperative FSO communications," *IEEE Trans. Wireless Commun.*, vol. 16, no. 12, pp. 8205–8219, Dec. 2017.

CHADI ABOU-RJEILY (Senior Member, IEEE) received the B.E. degree in electrical engineering from Lebanese University, Roumieh, Lebanon, in 2002, and the M.S. and Ph.D. degrees in electrical engineering from the École Nationale Supérieure des Télécommunications (ENST), Paris, France, in 2003 and 2006, respectively. He is a Professor with the Department of Electrical and Computer Engineering, Lebanese American University (LAU), Byblos, Lebanon. From September 2003 to February 2007, he was a Research Fellow with the Laboratory of Electronics and Information Technology, French Atomic Energy Commission (CEA-LETI). His research interests include code construction and transceiver design for wireless communication systems.